PRIMARY BREAKUP OF LIQUID SHEETS IN CROSSFLOW AND LIQUID JETS IN GASEOUS COFLOW

By

MUHAMMAD SAQIB RAZA

Bachelor of Science in Mechanical Engineering

Oklahoma State University

Stillwater, OK

2019

Submitted to the Faculty of the
Graduate College of the
Oklahoma State University
in partial fulfillment of
the requirements for
the Degree of
MASTER OF SCIENCE
May, 2022

PRIMARY BREAKUP OF LIQUID SHEETS IN CROSSFLOW AND LIQUID JETS IN GASEOUS COFLOW

Thesis Approved:

Dr. Khaled Sallam

Thesis Adviser

Dr. Arvind Santhanakrishnan

Dr. Brian Elbing

ACKNOWLEDGEMENTS

This Master's program at OSU has been a great experience. The company of people, faculty, staff, mentors, lab mates, groups I've been a part of and friends who were always there, without their help and support this thesis would not have been possible.

First and foremost, I would like to thank Dr. Sallam who served not only as my advisor but also as a great mentor who advised me through the entire undergraduate and graduate studies. It has been a pleasure working with him and learning a great deal of skills and life lessons. He has always been a motivation and pushed me through my entire coursework and was always available to help. I also would like to thank Dr. Brian Elbing and Dr. Arvind Santhanakrishnan for serving on my graduate committee and for their valuable feedback on this thesis.

The assistance in designing and assembling the present micro coflow injector by the New Product Development Center, Oklahoma State University, under the leadership of Dr. Robert Taylor, is gratefully acknowledged. I would also like to thank National Science Foundation (Program Director: Dr. Ruth Shuman) and John Zink Hamworthy Combustion Company for funding part of my education.

Last but not the least I would like to thank my parents and siblings for their continued efforts and support in my entire college life.

Acknowledgements reflect the views of the author and are not endorsed by committee members or Oklahoma State University.

Name: MUHAMMAD SAQIB RAZA

Date of Degree: MAY, 2022

Title of Study: PRIMARY BREAKUP OF LIQUID SHEETS IN CROSSFLOW AND LIQUID JETS IN GASEOUS COFLOW

Major Field: MECHANICAL AND AEROSPACE ENGINEERING

Abstract: This thesis discusses the breakup of liquid sheets under the influence of crossflow and the breakup of micro-liquid jets in coflow air. The breakup of liquid jets and sheets is important for many applications, e.g., agricultural sprays, fuel atomization, and spray coatings, nasal spray delivery, among others. The aerodynamic effects on the liquid breakup process are studied experimentally to identify the breakup regime transitions and droplet sizes. Two different setups were used to investigate experimentally the breakup process in both the crossflow and coflow configurations. A subsonic wind tunnel was used to simulate the crosswind effects on flat fan nozzle spray. Two flat fan nozzles were mounted at the ceiling of the test section of the wind tunnel. Rotameters, pitot tube, and inclined manometer were used to measure the flowrates and velocities, respectively. A micro coflow injector was constructed at the new product development center from two beveled needles (16G and 30G) one inside the other and were used to study breakup of micro liquid jet in with and without the presence of coflowing air.

A high-speed digital imaging technique was used in both setups to capture different breakup regimes and to measure the breakup regime transitions, the location of the end of the liquid core, the breakup time, the location, and the size of droplets at the onset of breakup and the spray trajectory. The effects of spray angle for flat fan nozzle spray and the aerodynamic effects on the spray outcomes are presented in this thesis. The results were correlated using phenomenological analyses. For liquid sheets in crossflow, the aerodynamic effects were responsible for initiating bag breakup and reducing the droplet sizes. which are susceptible to drift. This would be problematic for spraying herbicides in windy conditions. For the breakup of micro liquid jets in gaseous coflow the aerodynamic effects resulted in accelerating the breakup process and reducing the droplet sizes. The results show that the presence of air resulted in a large reduction of the droplet sizes compared with pressure atomization only. The effects of reducing the injector size on different measurements were obvious when compared with previous studies of larger coflowing injectors.

TABLE OF CONTENTS

Chapter Page

LIST OF TABLES

Table Page

LIST OF FIGURES

Figure Page

Figure Page

NOMENCLATURE

Parameters

A	Area at the nozzle exit [mm^2]
d_i	Droplet diameter at onset [μm]
d_L	Diameter of the liquid jet [mm]
L_c	Length of intact liquid core [mm]
P_{inj}	Injection pressure [psig]
q	Liquid-Gas momentum flux ratio ($q = \rho_L V_L^2 / \rho_G V_G^2$)
Q_L	Liquid flow rate [GPM]
r	Length of the sheet [m]
Re_L	Liquid Reynolds number ($Re_L = \rho_L V_L d_L / \mu$)
t	Thickness of the sheet [m]
t_b	Thickness at onset of bags [m]
t_d	Thickness at onset of drop [m]
t_e	Thickness at end of intact liquid core [m]
T_b	Time of breakup [sec]
T_R	Time for Rayleigh breakup [s]
T^*	Time of aerodynamic breakup [sec]
Y_b	Onset of bags [m]
Y_d	Onset of drops [m]
Y_e	End of intact liquid core [m]
U_G	Crossflow gas velocity [m/s]

V_L Vertical liquid velocity [m/s]

We_G Gaseous Weber number ($We_G = \rho_G V_G^2 d_L / \sigma$)

We_{GL} Weber number gas-liquid ($We_{GL} = \rho_G (V_G - V_L)^2 d_L / \sigma$)

We_L Liquid Weber number ($We_L = \rho_L V_L^2 d_L / \sigma$)

Greek Symbols:

θ_F Expansion fan angle [◦]

θ_D Jet deflection angle [◦]

μ Dynamic viscosity of water [Pa. s]

ρ_L Density of the liquid (Water) [kg/m^3]

ρ_G Density of the gas (Air) [kg/m^3]

σ Surface tension [N/m]

CHAPTER I

INTRODUCTION

1.1. Background

Atomizers are widely used in the industry as they have proven beneficial in many applications, e.g., agriculture, drug delivery, spray painting, combustion of liquid fuels. Aerodynamic forces (quantified by weber number (We) and momentum flux ratio (q)) play an important role in atomization. The role of aerodynamic forces could be planned, e.g., in Air-assisted atomizers which are useful for air breathing propulsion systems (e.g., afterburner, scramjet engines) due to their ability of producing larger penetration with comparatively small drop sizes. Alternatively, aerodynamic effects could be encountered as off-design conditions, e.g., agricultural spray drift due to crosswind (Fig. 1.1) or due to aerial herbicides and pesticides application. This study is concerned with the aerodynamic effects on the primary breakup of liquid sheets and round liquid jets

The primary breakup of liquid jets in still gases is characterized into four different regimes (Lin & Reitz, 1998) as shown in Fig. 1.2 by Bonhoeffer et al. (2017):

a) Rayleigh regime: this regime is encountered at low velocities. A cylindrical liquid jet is unstable when subjected to symmetrical instabilities. It breaks into uniform and big droplets (almost twice the diameter of the liquid jet). This region is dominated by the surface tension of the liquid.

b) First wind induced regime: this regime is encountered when the aerodynamic effects induce disturbances in the flow affecting the breakup mechanism. A sinusoidal wave pattern emerges, and the droplets are generated from the tip of the liquid jet (i.e., liquid core breakup) marking the end of the intact core length. The end of intact liquid core is the place where the liquid jet ceases to exist as a continuous jet and results in the formation of droplets known as the onset of droplets as shown in Fig. 1.3.

c) Second wind induced regime: this regime is encountered at higher liquid jet velocities. At the location of onset of breakup ligaments form along the jet surface (i.e., surface breakup), which break into droplets via the Rayleigh breakup or turbulent breakup (Sallam & Faeth, 2003), eventually breaking the jet as a whole due to surface breakup or it stops, and the jet is broken due to liquid core breakup. This regime produces smaller droplets compared to the previous two regimes.

d) Atomization regime: As the surface instabilities get more active, droplets are observed at the nozzle exit. The droplets produced in this regime are much smaller in size compared to all the other regimes.

Based on the application different spray characteristics are desired and hence it is crucial to understand the breakup process of liquid jets which leads to the formation of droplets as the jet disintegrates. For example, in cooling towers smaller droplets are desired to increase the surface area for better heat transfer etc. In agriculture where spray drift is a problem, optimum size droplets are desired, so they stick to the targeted area instead of bouncing, sliding on the crop or potentially being blown away by the crossflow wind. Recently an herbicide named Dicamba was banned due to its harmful effects on crops that were not genetically modified. This drifted spray is responsible for water pollution, effecting the quality of air in the surroundings area and hence decreasing the quality of life for the people residing around such areas.

Pressure atomized liquid jets are not enough to produce desired drops in some applications due to limitation of space (intact core length) or time (rates of breakup). The addition of air to the liquid jets results in producing much more smaller droplets with larger nozzle diameters. Air is used as way to disintegrate the jet much faster to achieve the desired outcomes especially in combustion applications. This addition of air is sometimes parallel to the jet with liquid being in the center and air on each side (Fig. 1.4) and at other times the jet comes out of the orifice as a mixture of air and liquid (aerated jets).

The breakup process of liquid jet in still air can be characterized as follows: The liquid injected into still air emanates as a solid jet piercing through the air as the surface tension forces dominate and the region is called jetting, as the flow rate increases the liquid experiences disturbances in the flow due to the turbulence happening inside the nozzle and this disturbance effects the liquid stream and the jet breaks up into big chunks separated from the main jet known as ligaments these ligaments are further broken down into finer droplets and hence completing the atomization process.

In the presence of crossflow air, the regimes of flat fan spray are characterized as dripping, jetting, sheet breakup, and bag breakup respectively. The fan spray angle as shown in Fig. 1.5 plays a crucial role in determining the regime transitions as will be discussed in chapter 2. The aerodynamic forces were quantified by Weber number (We) defined as the ratio between inertial forces and surface tension forces and momentum flux ratio (q) defined as the ratio between liquid – gas momentum flux, and are described as follows:

$$q = \rho_L V_L^2 / \rho_G V_G^2 \tag{1.1}$$

$$We_G = \rho_G V_G^2 d_L / \sigma \tag{1.2}$$

$$We_{GL} = \rho_G (V_G - V_L)^2 d_L / \sigma \tag{1.3}$$

1.2 Problem Statement

Aerodynamic forces play a major role in the primary breakup mechanism of liquid sheets and liquid jets. This could lead to either optimum droplet size distribution or in certain configuration leads to undesirable breakup outcomes (size distribution, spatial distribution, and the end of intact liquid core). Of concern in the present work, is the breakup regime transitions due to the aerodynamic forces for two specific configurations: liquid sheet in crossflow and liquid jet in gaseous coflow.

1.3 Specific Objectives

The objectives of this research were as follows:

1. Identify the primary breakup regimes of a liquid sheet in crossflow and construct a breakup regime transition map under crossflow wind conditions to identify the transition between bag and sheet breakup.
2. Investigate the effect of the liquid flow rate on the expansion of the liquid sheet fan angle and formulate a phenomenological theory for the sheet thickness.
3. To understand the breakup behavior of liquid sheet in crossflow and develop a theory for the elimination of bag formation that are susceptible to drift.
4. To investigate the onset of drops, onset of bags, end of intact liquid core, time of breakup, and trajectory of the jet in crossflow based on jetting, sheet, and bag breakup regimes.
5. To investigate the effects of coflow air on the breakup of the liquid jet.
6. To investigate the end of intact liquid core, time of breakup, and droplet diameter at the onset of drops.

1.4 Organization of the thesis

In chapter 1 the background, the problem statement, and the specific objectives of the present study are presented. The Aerodynamic breakup of Liquid Sheet in Crossflow is discussed in

chapter 2. The Aerodynamic breakup of Liquid Jet in gaseous Coflow is discussed in chapter 3. Finally, the summary, conclusions, and recommendation for future work are presented in chapter 4.

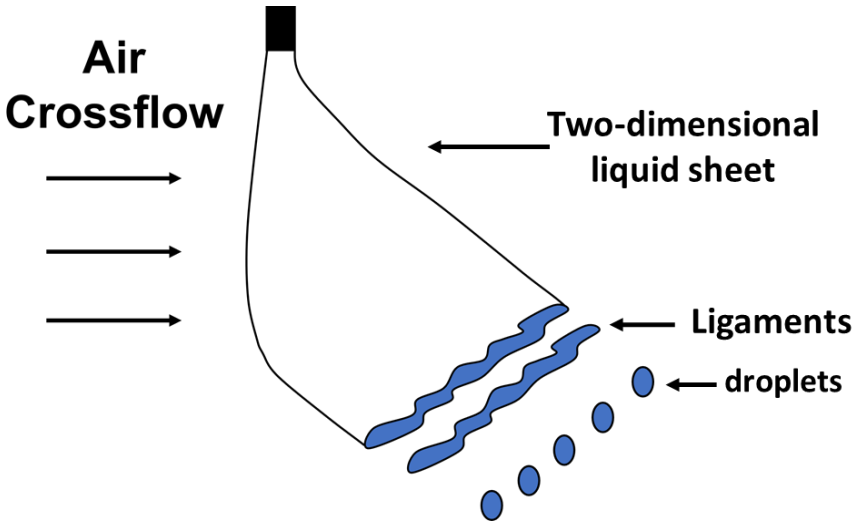

Fig. 1.1 Liquid sheet disintegration subjected to crossflow wind.

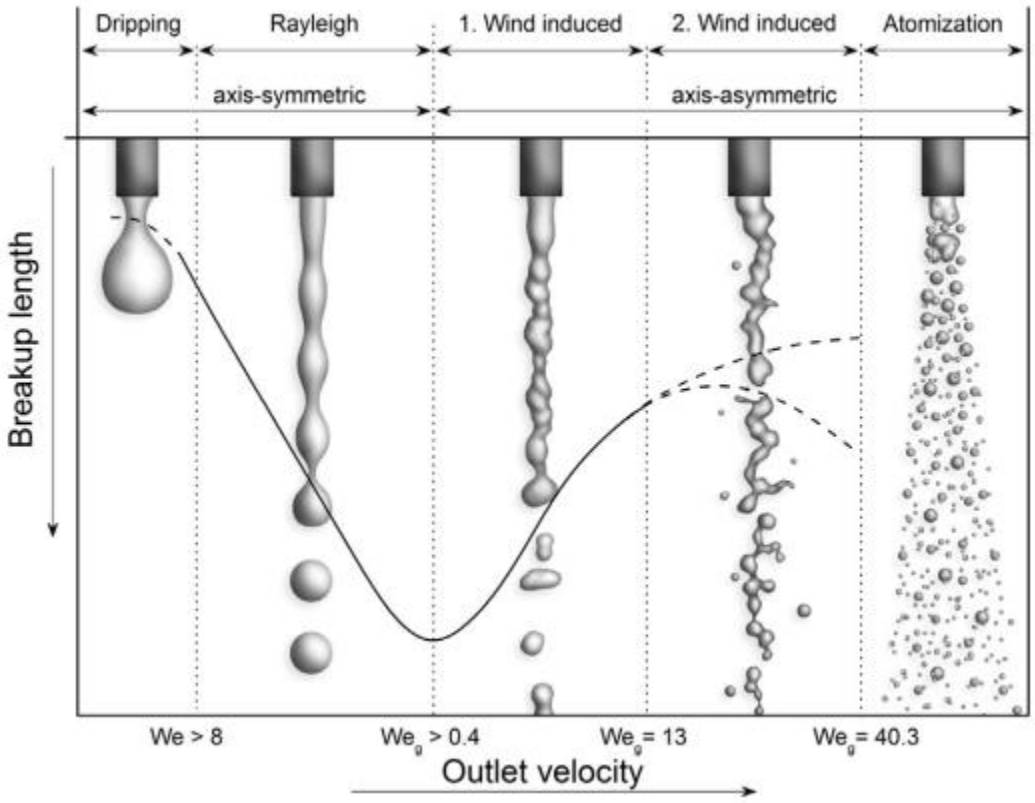

Fig. 1.2 Breakup regime map for round liquid jet in still air as a function of increasing liquid velocities (Bonhoeffer et al., 2017).

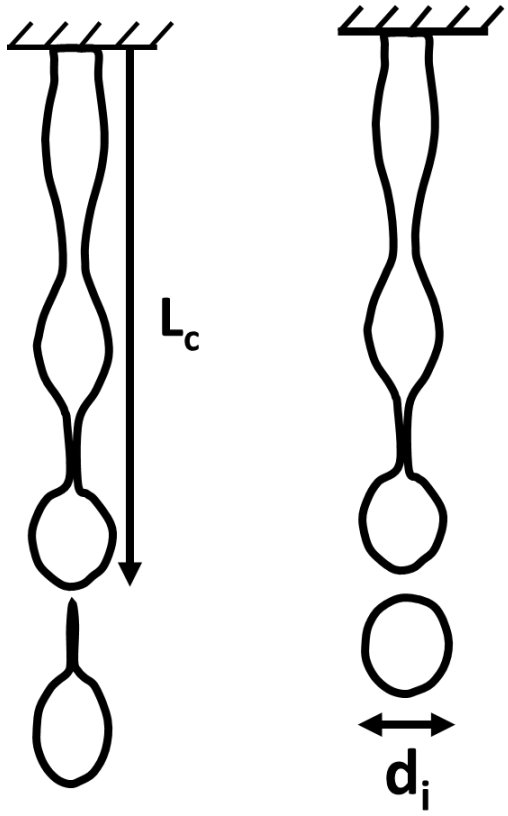

Fig. 1.3 The end of intact liquid, L_C, and droplet diameter at onset, d_i.

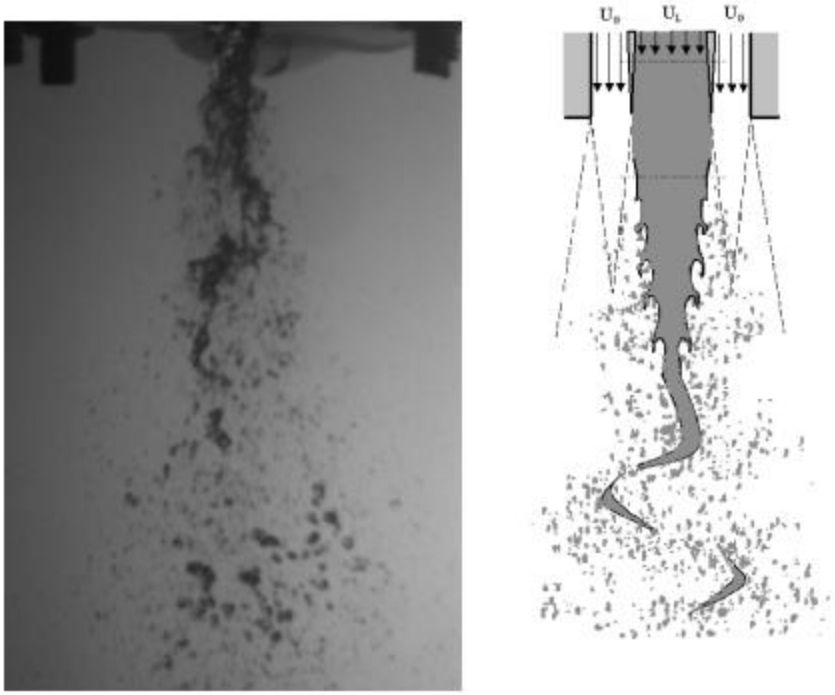

Fig. 1.4 Coflow jet breakup due to air induced instability (Matas & Cartellier, 2006).

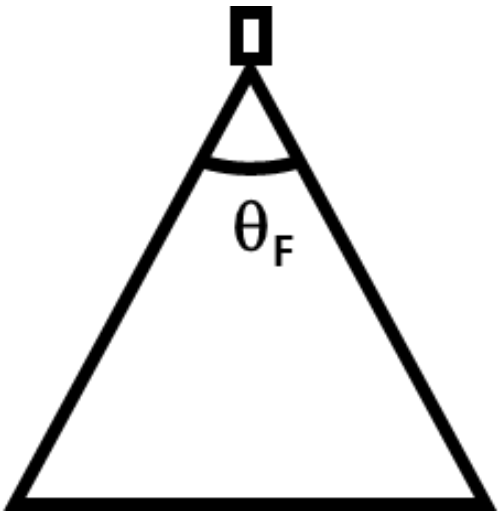

Fig. 1.5 Fan spray angle, θ_F.

CHAPTER II

PRIMARY BREAKUP OF LIQUID SHEETS IN CROSSFLOW

2.1 Introduction:

The goal of this work is to study the primary breakup of liquid sheets injected from flat fan nozzle into gaseous crossflow motivated by applications to drift of agricultural sprays. Spray drift is a troublesome problem for spraying applications as it effects not only the crops but also leads to poor quality of air, contaminated water which effects farmers as well as people living nearby these fields. Several studies have been conducted on spray drift. Yarpuz-Bozdogan and Bozdogan (2009) studied the atomization outcomes from different nozzles and found that using the correct nozzle type can significantly reduce the bystander (people living around the spraying areas) exposure by 21 - 47%. Flat fan nozzle has been used for several industrial and agricultural applications such as absorption chillers, pesticide, and herbicide applications (Zacarias et al., 2011, Derksen et al., 2008, Ellis et al., 1997, Bueno et al., 2016, Holland et al., 1997, Zhong et al., 2003, Dukes et al., 2004, Sikkema et al., 2008, Egan et al., 2014, Uremis et al., 2004, Wang et al., 2010, among others). The typical breakup mechanism of the flat fan nozzle in still air involves the expansion of the liquid jet injected from an elliptical nozzle exit to form a thin liquid sheet, followed by the disintegration of the sheet into fine ligaments (Altieri et al., 2014). The ligaments would then undergo Rayleigh breakup to form the spray droplets. In applications where targeted delivery is desired, optimum drops sizes are crucial. Larger droplets are not effective in the treatment of crops as suggested by (Doll et al. 2005).

This could be explained by the weight of the droplets; heavier droplets are susceptible to bounce from the crop and hence are ineffective in the treatment of crops. Hewitt (2008) studied flat fan nozzles for aerial applications and found that at higher pressures the outcome from a small orifice flat fan nozzle is unaffected by the crosswind resulting in similar droplet sizes as in no wind conditions. He also observed the dependence of spray angle on the outcome of the drop sizes, with larger angles producing smaller drop sizes and vice-versa. This effect is related to the thickness of the sheet being formed, larger fan angle results in expanding of the sheet which results in a thinner sheet (weakening the surface tension) and as the sheet disintegrates into ligaments smaller droplets are produced, however, for narrower angles larger ligaments are formed and hence large droplets as discussed by (Ellis et al. 1997). The presence of surfactant, emulsion, and polymer adjuvants affect the formation of sprays from flat fan nozzle (Miller et al., 2001). The use of emulsions and surfactants is a common practice for spraying pesticides and herbicides in agriculture applications to achieve the desired fluid characteristics, and spraying characteristics, e.g., to enhance the sheet length or to disintegrate the sheet much closer to the nozzle exit (Miller and Ellis, 2000, Dexter, 2001, Thompson and Rothstein, 2007). Water soluble surfactants show almost the same behavior as water and tend to show higher drift potential whereas emulsions reduce drift as they produce much coarser drops that can withstand the wind. Dexter (2001) reported that hole growth and concave (contracted inwards) fan angle were not seen in water. A concern, however, is that at higher flow rates, holes may start to form and lead to sheet disintegration. The quality of atomization affects the susceptibility of herbicides to crosswind drift. Of concern is the effect of the crossflow (side wind) on the breakup regime transitions and the quality of the atomization. When the flat fan nozzle is used in windy conditions (crossflow) one would observe smaller drop sizes. The effect of crossflow on the breakup of round liquid jets is well studied (Sallam et al, 2004). Jadidi et al. (2018) reported that elliptical jets are prone to early breakup compared to round liquids jets, this could be explained by the growth of instabilities in the elliptical jets much closer to the nozzle exit that expedite the

breakup process. Jadidi et al. (2018) also observed a weak penetration power of the elliptical jets into the crossflow compared to the round jets as round jets are exempted from axis-switching phenomenon and hence produce higher penetration into the crossflow. The breakup of flat fan nozzle spray in a gaseous crossflow is more complicated due to the competition between the two primary breakup mechanisms; (a) sheet breakup caused by the continuous thinning of the liquid sheet due to the expansion angle (Wang et al., 2019) and (b) the aerodynamic breakup caused by the presence external crossflow as well as the relative wind velocity due the large liquid injection velocity. This is followed by secondary breakup, wherein drops formed through the first step break up into smaller ones due to aerodynamic forces.

Unfortunately, not enough studies have been performed to eliminate the root cause of spray drift in agricultural applications. In the present study high speed imaging is used to extend recent studies of jets in subsonic crossflow and flat fan nozzle breakup in still air to characterize the effects of crossflow on the primary breakup regimes transitions and the spray outcomes of flat fan nozzle spray. The present study focuses on the effect of the crosswind velocity on the breakup characteristics of two different flat fan nozzles sizes to characterize the phenomenon that results in the formation of drift-susceptible droplets, and to understand the physics of bag development under the influence of crossflow wind, typical of spraying herbicides in agricultural applications.

2.2 Experimental Methods:

The primary breakup of the liquid sheet from two different nozzles when subjected to crossflow was investigated experimentally using high speed imaging.

2.2.1 Apparatus:

Two flat fan nozzles (Smith 182932 Poly Fan Nozzle kit), shown in Fig. 2.1, were used to generate the spray inside the test section of a subsonic wind tunnel. The 1.5 mm diameter poly flat fan nozzle (high flow nozzle) was rated as 0.25 GPM, 70-degree fan, whereas the 1 mm

diameter poly flat fan nozzle (low flow nozzle) was rated as 0.15 GPM, 30-degree fan. The cross-section area of both nozzles was measured from the images shown in Fig. 2.1, as 1.77 mm^2 and 0.8 mm^2, for the high flow and low flow nozzles, respectively. An equivalent diameter, d_L, based on the same cross-sectional area as the nozzle was calculated and used in the present study to calculate the Weber number and normalize the spatial measurements of the onset of bag and onset drop breakup as well as the end of the liquid core. The experiments were conducted in the test section of a subsonic wind tunnel as shown in Fig. 2.1. The test section had a maximum air velocity of 60 m/s and its cross-section area was 1 ft by 1 ft. The test liquid was contained within a cylindrical test chamber constructed form 304 stainless steel. The test liquid was placed within the test section using the liquid fill line, shown in Fig. 2.1. Pressurized air from a large air tank (1.3 m^3) maintained at constant pressure was used to pressurize the test liquid. Excessive aeration of the test liquid during liquid injection was prevented using a baffle across the air inlet of the test chamber. This arrangement provided a test time less than a minute for each test condition. This was not problematic, however, since the current diagnostics (high speed imaging) only needed a total of 1 sec to record 5000 frames.

The liquid was metered after leaving the test chamber by an inline rotameter, not shown in Fig. 2.1, for simplicity, before flowing to the injection flat fan nozzle inserted at 90^o inside the test section of the wind tunnel, i.e., normal to the air flow direction. The flat fan nozzle was oriented such that the generated sheet was normal to the crossflow. However, when the fan angle was measured, the fan nozzle was rotated so that the liquid sheet is normal to the camera, i.e., it was parallel to the flow direction, as shown in Fig. 2.2 & 2.3.

2.2.2. Instrumentation:

The near injector region is critical to understanding primary breakup mechanism. A challenging aspect of investigating this region is that droplets are mostly non-spherical, which

makes this region inaccessible for measurement techniques such as PDA that rely upon the sphericity criterion. An imaging technique, e.g., shadowgraphy, on the other hand is not limited to spherical droplets, and it would provide more useful information about the spray structure and the drop size distributions in the near injector region. In the present study back-light illumination was used with a high-speed camera (XS4, 5000 fps at 500 pixels x 500 pixels). The spray images were analyzed using ImageJ software by using the following 3 steps; 1) The images were loaded as stacks into the program, 2) nozzle outer diameter was used to calibrate the images 3) the images were then converted into black and white with edges, so a clear edge is visible for consistent measurements. Each test condition was recorded using 5000 frames. The images were spatially calibrated by measuring the distance across the nozzle cap shown in each image. The present resolution of measuring the location of the onset of drop was 0.2 mm. The air speed in the wind tunnel was measured by a pitot static tube and an inclined manometer. The uncertainty in measuring the wind speed was 0.12 m/s. The volumetric flowrate to the nozzle was measured using rotameter tubes (Omega Engineering). The resolution of measuring the volumetric flow rate was 9 cm^3/min. All the measurements were restricted to within 10% of the statistical uncertainty of 95% confidence interval.

2.2.3. Test Conditions:

The current study was limited to water as the test liquid. To quantify the aerodynamic effects on the breakup of liquid sheet, test conditions included air crossflow as well as no crossflow conditions, which was important to understand the breakup mechanism in the absence of crossflow wind and allowed the measurement of spray angle. To study the effects of air crossflow on the breakup of liquid sheets four different air velocities were used and at each air velocity 4 different liquid flow rates were tested. The air velocity used in the current study ranged from 0-46 m/s. The higher velocity was selected to simulate the aerial spraying applications of herbicides. The test conditions are summarized in Table. 2.1.

2.3. Results and Discussion:

2.3.1. Liquid sheet in still air:

Flow visualization for the 1.5 mm nozzle (Fig. 2.2) showed the formation of sheet with rims at the edges like the observation of Dombrowski and Fraser (1954) and Clark and Dombrowski (1972). As the flow rate increases from left to right in Fig. 2.2, the expansion of the sheet is observed because of higher pressures. At lower flow rates the surface tension force dominates and the sheet contracts towards the axis of sheet as discussed by Dombrowski and Fraser (1954). For higher flow rates the sheet emanates in the radial direction at first and then the surface tension forces tend to contract it inwards towards the sheet axis, forming ligaments followed by droplets from the side. The sheet is unable to contract fully and breaks as a whole as the contraction from the left and right rim edges meet each other. At relatively higher flow rates for 1.5 mm nozzle (Fig. 2.2), holes were formed inside the sheet which grow further downstream and ultimately leading to breakup of the sheet like the observation of rectangular jets (Jaberi and Tadjfar, 2020), and elliptical jets (Altieri et al., 2014). Visual inspection of the sheet showed that these holes were formed in the near nozzle region because of disturbances inside the nozzle (Dombrowski and Fraser, 1954). However, Altieri et al. (2014) predicted that the presence of another immiscible phase might be the cause of hole formation.

The flow visualization for the 1 mm nozzle (Fig. 2.3) showed disintegration of the sheet only from the middle of the sheet instead of the rims with surface waves being the main mechanism of disintegration (Clark and Dombrowski, 1972). At higher flow rates the sheet expanded similar to the flow pattern predicted by Dombrowski et al. (1960). The interesting phenomena of axis switching is shown in Fig. 2.4. It was also observed for rectangular jets (Jaberi and Tadjfar, 2020, Zhang et al., 2021) and for elliptical jets (Kasyap et al., 2008). As the jet exits the nozzle two rims are formed on the edges contracted inwards connected by a thin sheet like the 1.5 mm nozzle

(Fig. 2.2) because of surface tension forces, the rims then collide and form a sheet in the normal direction. This repeats until the jet breaks into droplets. The calibration of the fan angle was performed for the two nozzles. The fan angle was measured by orienting the fan normal to the camera view, i.e., parallel to the wind tunnel flow, as shown in Fig. 2.2 & 2.3. The fan angle was measured form the images using ImageJ software. The fan angle was plotted as function of the liquid flow rate as shown in Fig. 2.5, and following correlations were obtained with correlation coefficients of R = 1 for both diameter nozzles respectively.

$$\theta_F = 17 \ln (Q_L) + 93.7 \quad (2.1)$$

$$\theta_F = 19.5 \ln (Q_L) + 90 \quad (2.2)$$

The fan angles of the two nozzles were correlated with the flow rate for the present test range. The high flow nozzle achieved the rated fan angle of 70^o at the rated flow rate of 0.25 GPM whereas the small flow nozzle expanded to 60^o rather than the rated 30^o at the rated flow rate of 0.15 GPM. This was not problematic, however, for the scope of the current study and the two nozzles used.

2.3.2. Liquid sheets in crossflow:

Visual representation of the liquid sheet breakup at an air velocity of 10.4 m/s is shown Fig. 2.6. The breakup regime observed were dripping (Fig. 2.6a) (formation of spherical drops at the tip as the liquid emerges from the tip), jetting defined as continuous homogenous stream of liquid (Fig, 2.6b) resulting in drops from Rayleigh-Taylor (RT) instability, followed by sheet breakup (Fig. 2.6c) and then formation of aerodynamic bags. At higher crossflow (Fig. 2.6d) three different regions are observed for the jet in crossflow named as regions R1, R2 and R3 respectively. R1 (bag breakup) is the region corresponding to small drops formed as the aerodynamic forces push through the thin sheet blowing bags which ultimately burst into very tiny droplets and are easily carried by the wind (i.e., spray drift). R2 (sheet breakup) corresponds

to the middle region of the spray where the droplets are formed in the direction of spray after sheet disintegrates into ligaments and R3 (rim breakup) corresponds to the region of the drops that are formed because of Rayleigh-Taylor instability from the side ligaments and are larger than both regions R1 and R2. The effect of crossflow velocity was also observed as shown in Fig. 2.7 by keeping the liquid velocity constant and varying the crossflow velocities. The regimes transitioned from jetting (Fig. 2.7a), sheet breakup (Fig. 2.7b) to bag breakup (Fig. 2.7c) and then dripping (Fig. 2.7d). However, this dripping is due to the fact that aerodynamic forces are so dominant, and the liquid doesn't have the chance to form a jet and breaks very close to the nozzle.

2.3.3. Breakup Regimes:

A breakup regime map was constructed by varying the nozzle flow rate for different crossflow velocities and characterized into 5 different regimes (dripping, jetting, sheet, bags, and sheet/bags). The breakup regime map was plotted for the present test conditions using the crossflow Weber number on the Y-axis and the momentum flux ratio on the X-axis as shown in Fig. 2.8. The breakup map may seem surprising since the bag breakup tend to be associated with larger volumetric flow rate, and hence higher q values, for the same crossflow Weber numbers. This is plausible because higher q values result in larger fan expansion and the establishment of a thin sheet that is more susceptible to bag breakup. The presence of side wind (i.e., crossflow), typical of spraying in windy conditions or aerial spraying would deflect the spray in the downwind direction, as shown in Fig. 2.6. In the case of sheet breakup, as shown in Fig. 2.6.c., strong wind conditions result in the triggering of a new breakup regime: termed here bag breakup of liquid sheets as shown in Fig. 2.7.d. The bag breakup of liquid sheet in crossflow would be problematic for agricultural sprays since the breakup of bags are associated with fine droplets formation due the breakup of the bag membrane as observed in previous studies of bag breakup or round liquid jets in crossflow (Mazallon et al., 1999, Sallam et al. 2004, Aalburg et al., 2005).

It is therefore strongly recommended to avoid spraying herbicides in crossflow with similar test conditions.

In the present study two different phenomena were responsible for the formation of bags, as follows: 1) the flapping instability forming bags at higher flow rates (A.4.). The instability produced spiral-like bags which ultimately busted into finer droplets in the plane of the jet. The formation of spiral like bags have also been observed for elliptical jets (Broumand et al., 2021) and for turbulent round liquid jet in still air (Sallam et al., 2002). 2) Aerodynamic forces due to the crossflow acting normal to the sheet resulting in bag formation. The aerodynamic forces act on the sheet and ultimately blow bags which results in the formation of finer droplets following the process of bag breakup and are drifted in the normal direction to the jet plane (Jaberi and Tadjfar, 2020).

2.3.4. Onset of breakup and end of intact liquid core:

Onset of bags, drops and end of intact liquid core were measured for two breakup regimes, sheet, and bags. The distance for onset was normalized by the jet diameter and plotted against the momentum flux ratio, q, in Fig. 2.9) as well as 1/q (Fig. 2.10). As q increased (decreasing crossflow) the bags, drops and intact liquid core showed an increasing trend and eventually tend to settle down approaching the onset of no crossflow which is not shown in this graph. Another graph for onset vs 1/q was plotted in (Fig. 2.10) so that zero crossflow could be plotted. Due to the limitation of the Field of view (FOV) the onset of drops and end of liquid core were not measured. The of bags were consistently seen and measured, however. A line has been drawn to show the crossflow bags approaching to the average value of non-crossflow bags (Fig. 2.11), showing that in the absence of crossflow these bags will be observed. The correlations for the onset of bags, drops and end of intact liquid core vs q were obtained with correlation coefficients of 0.8, 0.9 and 0.95 respectively, as follows:

$$Y_b / d_L = 1.7\ q^{0.3} \quad (2.3)$$

$$Y_d / d_L = 1.5\ q^{0.4} \quad (2.4)$$

$$Y_e / d_L = 3.7\ q^{0.32} \quad (2.5)$$

Following the analysis of Sallam et al. (2004) for liquid jets in crossflow, Y_e/d_L, should scale with $q^{1/2}$. In the present study, the end of the liquid core scale with $q^{0.3}$, probably due to the sheet expansion effect on accelerating the end of the liquid core.

The dimensionless time of breakup (T_b/T^*) was plotted as function of the crossflow weber number (WeG). The breakup time for current study aligns well with the breakup time for round liquid jet in still air (Lee & Sallam, 2017) and for round liquid jet in crossflow (Sallam et al., 2004). A constant line has been drawn at 2.3 as shown in Fig. 2.12. The correlation has also been obtained with a correlation coefficient of 0.04, due to sampling limitation, and is given as follows:

$$T_b/T^* = 2.2\ We_G^{-0.01} \quad (2.6)$$

2.3.5. Sheet thickness:

Sheet thickness is an important parameter for the breakup of fan spray as it has direct relation with the quality of atomization. Sheet thickness was estimated by applying the continuity equation between the nozzle exit and the liquid sheet breakup location, as follows:

$$t = A / (r\ \theta_F) \quad (2.7)$$

Using the relation one can estimate t_b (thickness at onset of bags), t_d (thickness at onset of drops), t_e (thickness at end of intact liquid core). They were plotted against q as dimensionless parameters (Fig. 2.13). A decreasing trend in the thickness is seen as q increases. A transition line is drawn to show the presence of two different breakup mechanisms 1) bag breakup at lower q values. At smaller q values thicker sheet is observed which means strong crossflow is needed to penetrate a

thicker sheet. 2) Sheet breakup with flapping bags. This breakup mechanism is like the no crossflow bags as the effect of crossflow is negligible and bags are formed because of flapping instability as was also observed by Broumand et al., (2021).

The relation in Eq. (7) also shows the dependence of theta on the sheet thickness. The sheet thickness varies inversely with the fan angle. The higher the angle smaller will be the thickness and vice versa.

2.3.6. Jet Trajectory:

The jet trajectory data was plotted as dimensionless parameters where y / d_L*q was scaled with $x/d_L *q$ on a log-log scale. The trajectory for three regimes (jetting, sheet, and bags) was plotted as shown in Fig. 2.14. Power law correlations were obtained with correlation coefficients of 0.8, 0.92, 0.94 representing trajectory for jetting, sheet, and bags, respectively, and are given as:

$$y / (d_L\, q) = 0.8\ \ (x / (d_L\, q))^{0.57} \tag{2.8}$$

$$y / (d_L\, q) = 0.7\ \ (x / (d_L\, q))^{0.56} \tag{2.9}$$

$$y / (d_L\, q) = 2.5\ \ (x / (d_L\, q))^{0.9} \tag{2.10}$$

2.4. Conclusions:

The major conclusions for the study the breakup characteristics of liquid sheet injected from flat fan nozzles in crossflow wind are as follows:

1. The fan angle of the liquid sheet is controlled by the liquid flow rate at low flow rate before reaching its rated fan angle at the rated flowrate.
2. The crossflow can change the primary breakup mechanism from sheet breakup regime to bag breakup regime. Those bag structures break into smaller drop sizes than the drops resulting from the sheet breakup which results in an increased spray drift flux in

crosswind. The breakup regime transition from sheet to bag breakup is triggered when the momentum flux ratio, q, becomes smaller than 200.

3. Flapping bag breakup was observed at higher liquid flow rates due to surface instability. Those bags, observed previously at no crossflow condition, do not get stretched large enough to dominate the breakup mechanism of the liquid sheet.
4. The dimensionless breakup time for sheet and bag breakup is independent of the nozzle diameter and crossflow Weber number.

Table. 2.1 Test conditions for crossflow experiment

Parameters	Value
Liquid density, ρ_L [kg/m^3]	997
Gas density, ρ_G [kg/m^3]	1.23
Surface tension, σ [N/m]	0.072
Jet exit diameter, d_L [mm]	1, 1.5
Liquid-Gas momentum ratio, q [-]	5 - 18050
Liquid Weber number, We_L [-]	13 - 14486
Gas Weber number, We_G [-]	0.3 - 55
Gas Velocity, U_G [m/s]	4 - 46
Liquid Velocity, V_L [m/s]	1 - 21

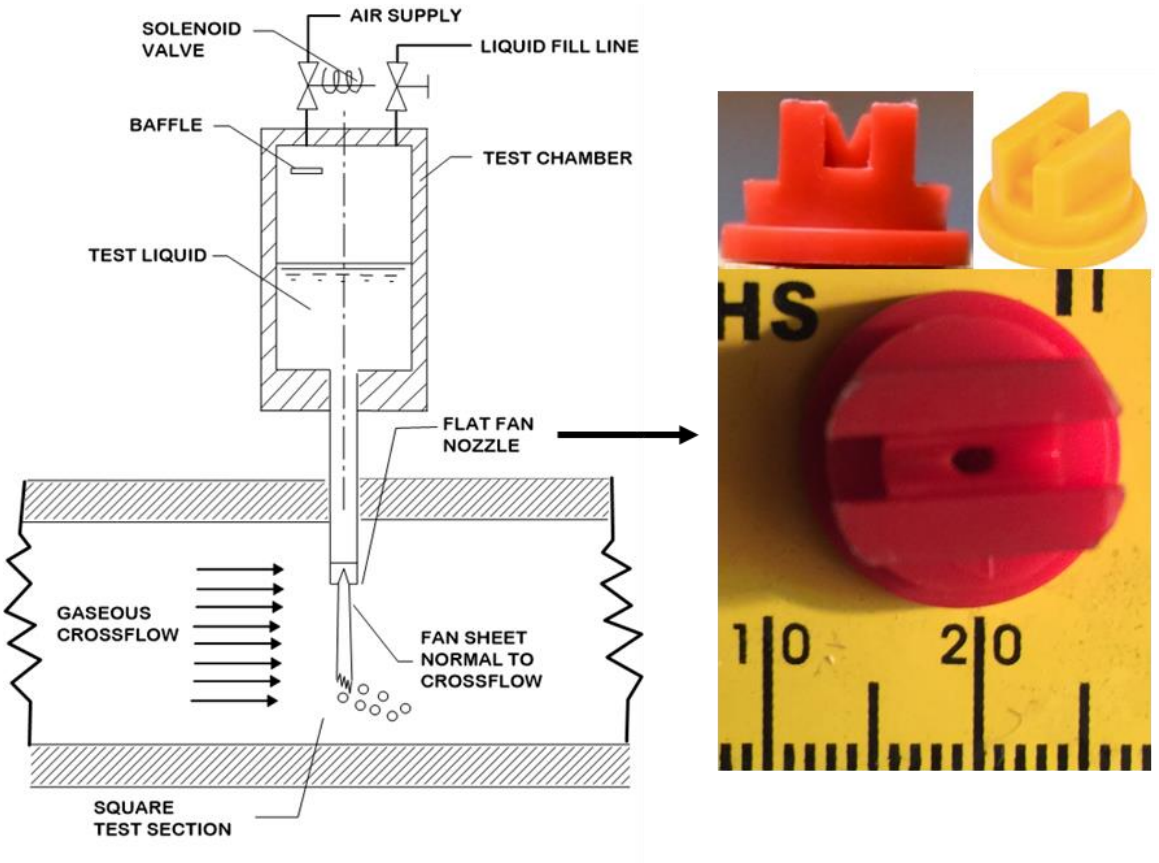

Figure 2.1. Apparatus with the flat fan nozzles used in the current study for crossflow experiment.

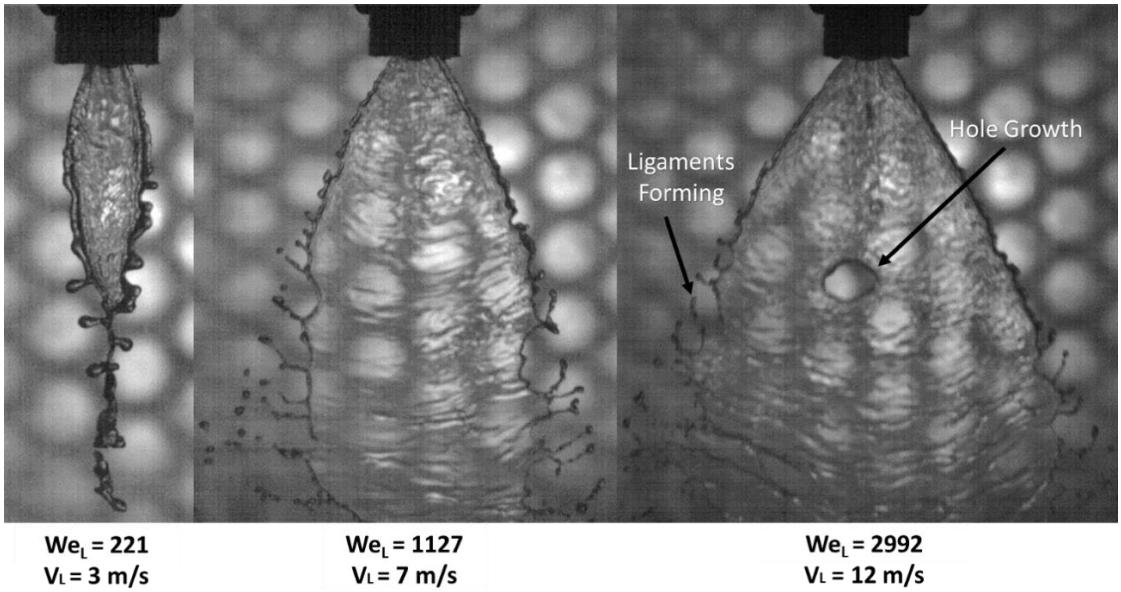

Figure 2.2. Visualization of spreading fan angle (d_L = 1.5 mm nozzle) in still air at three different liquid velocities with nozzle oriented parallel to the wind tunnel.

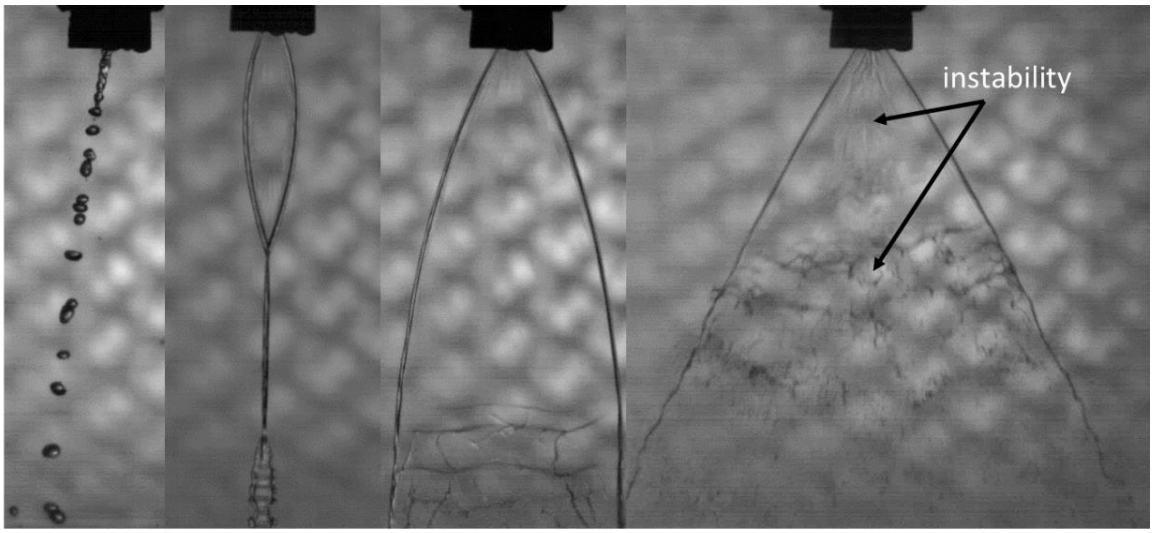

Figure 2.3. Visualization of spreading fan angle (d_L = 1 mm nozzle) in still air at four different liquid velocities with nozzle oriented parallel to the wind tunnel.

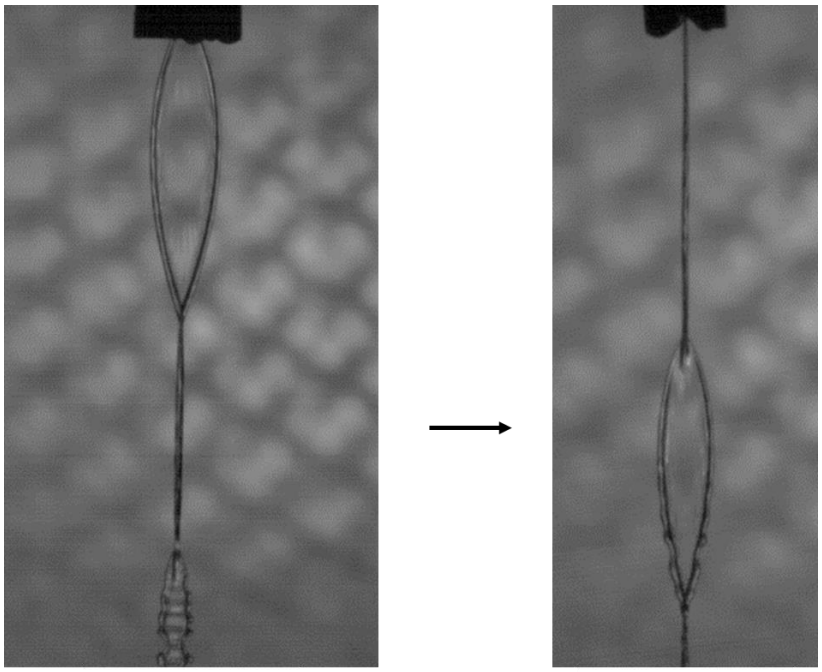

Figure 2.4. Visualization of axis switching phenomena observed in current study, left (front view) and right (side view).

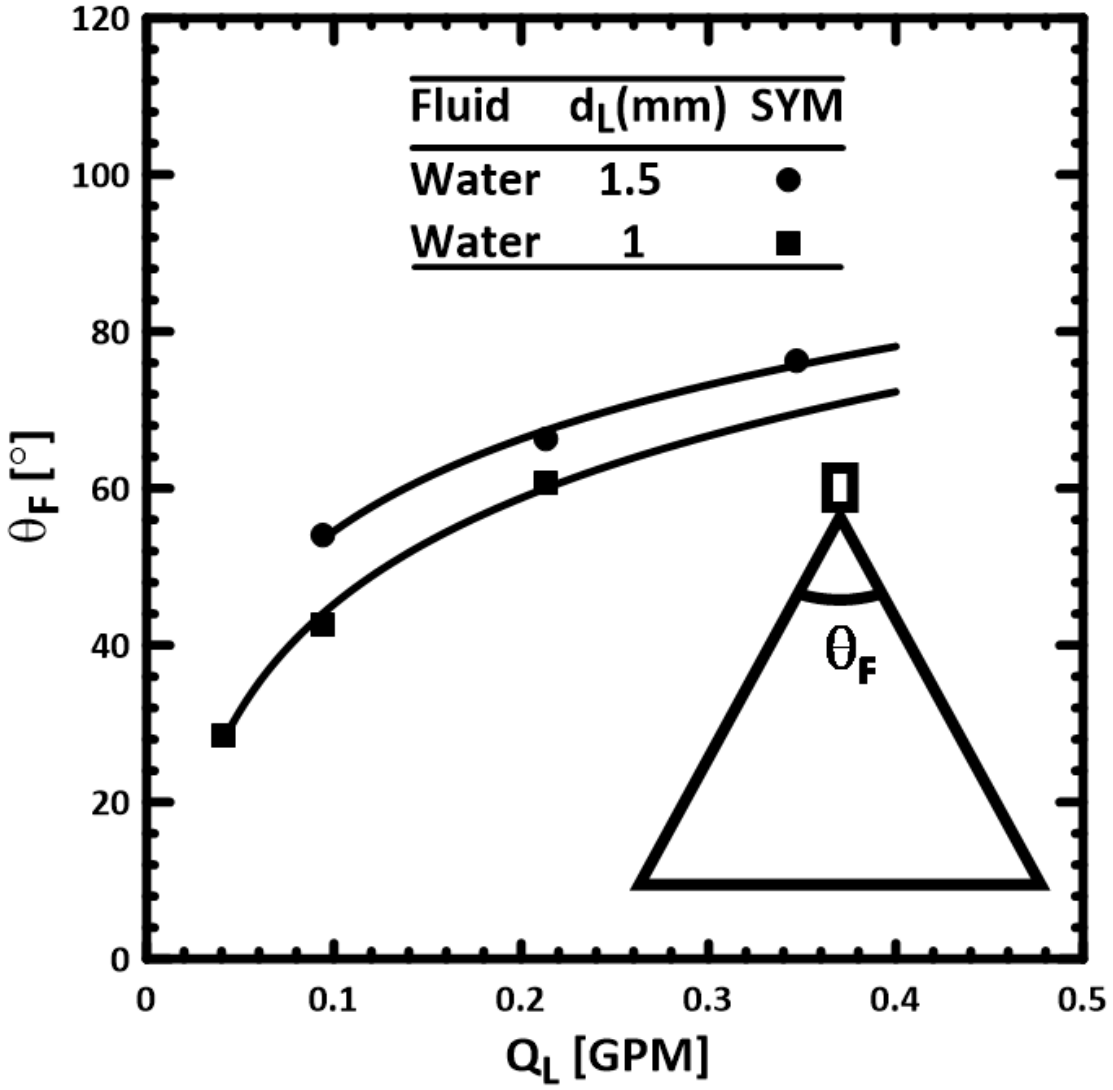

Figure 2.5. Variation of Fan angle as a function of the flowrate for the two flat fan nozzles used in the present study.

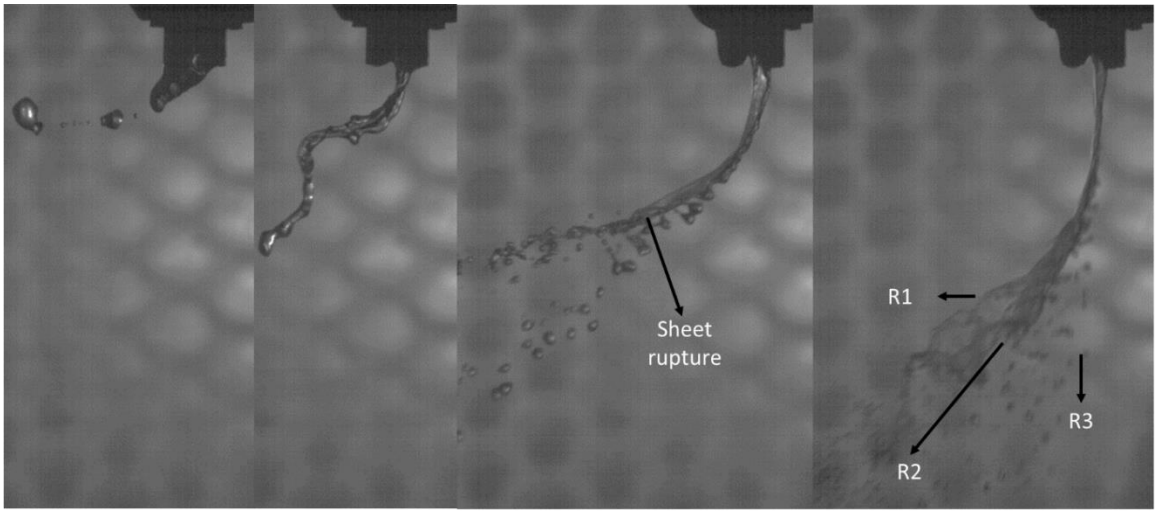

Figure 2.6. Breakup regime visualization showing the effect of jet velocity for the (d_L = 1.5 mm) nozzle at a crossflow (wind blowing from right to left) velocity of 10.4 m/s.

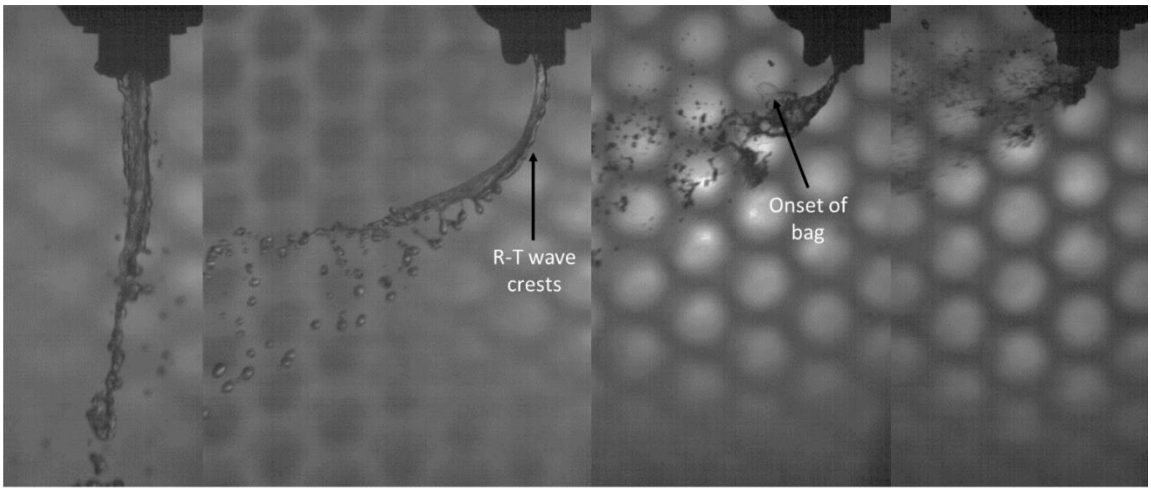

Figure 2.7. Effect of crossflow velocities on flat fan spray (d_L = 1.5 mm nozzle). Test conditions: Liquid exit velocity is 3 m/s.

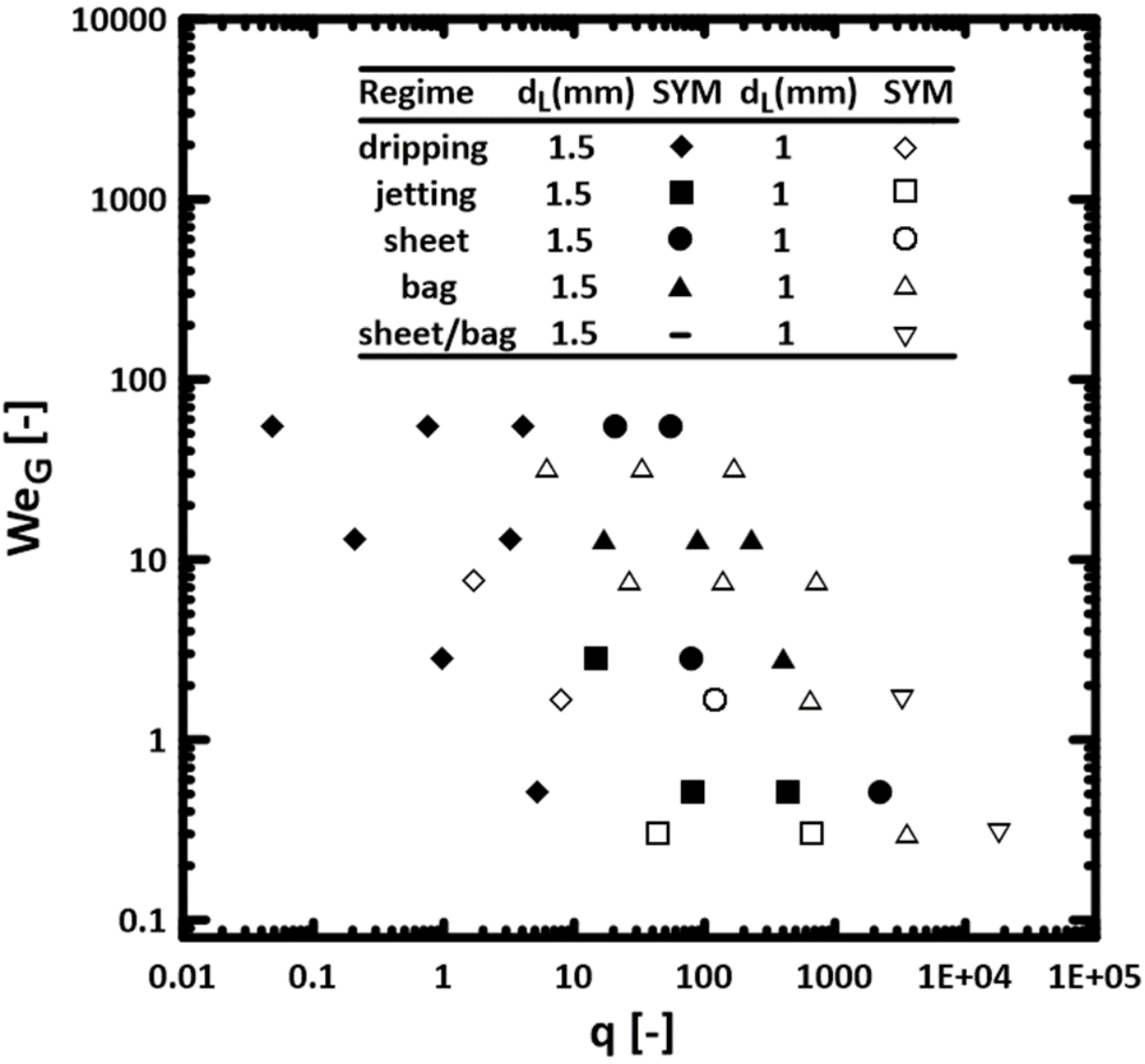

Figure 2.8. Breakup regime map for flat fan nozzles in crossflow fan nozzles (d_L = 1.5 mm and 1 mm) as function of momentum flux ratio.

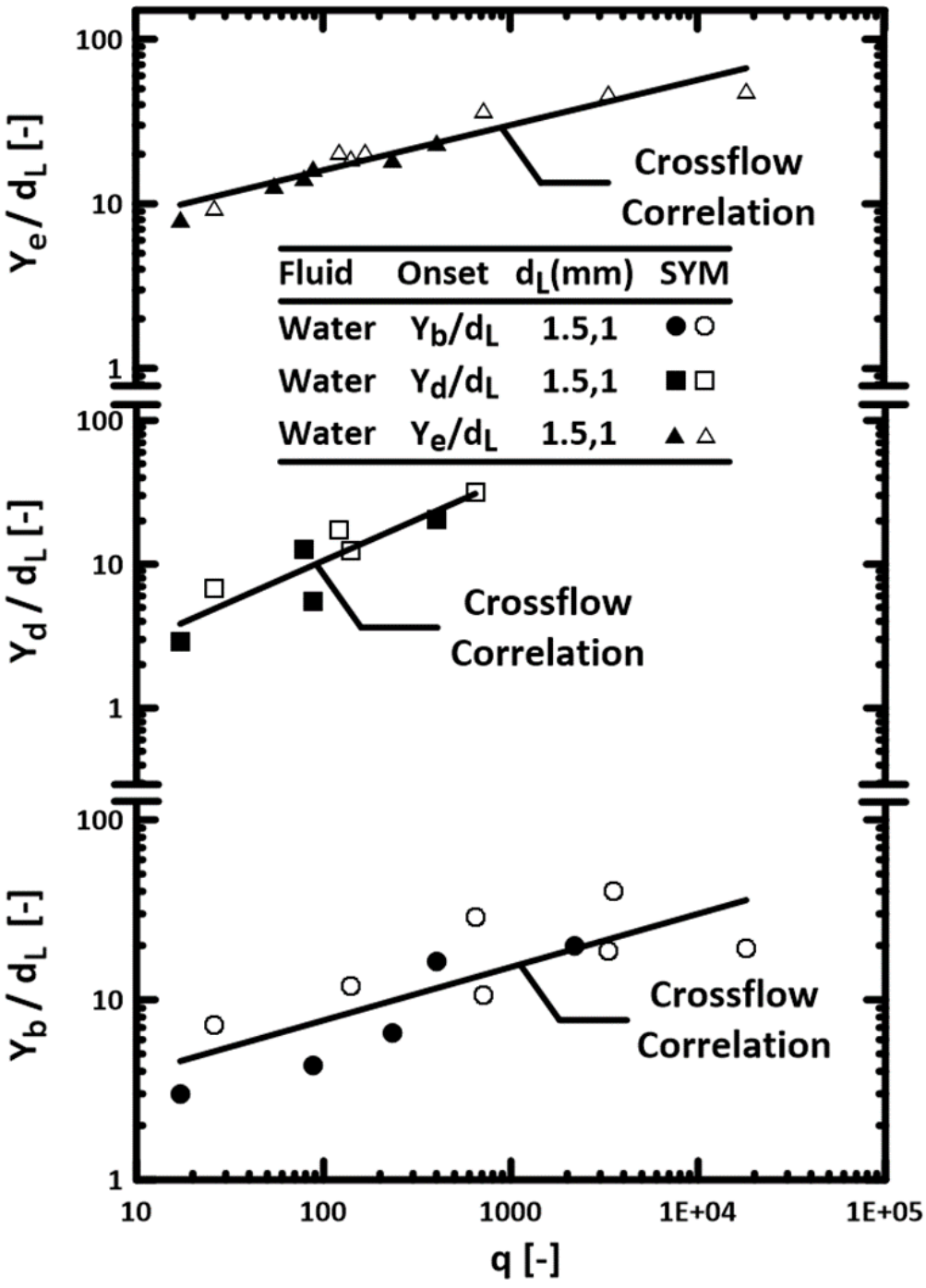

Figure 2.9. Onset of bag, drop and end of liquid core for fan nozzles (d_L = 1.5 mm and 1 mm) as function of momentum flux ratio, q.

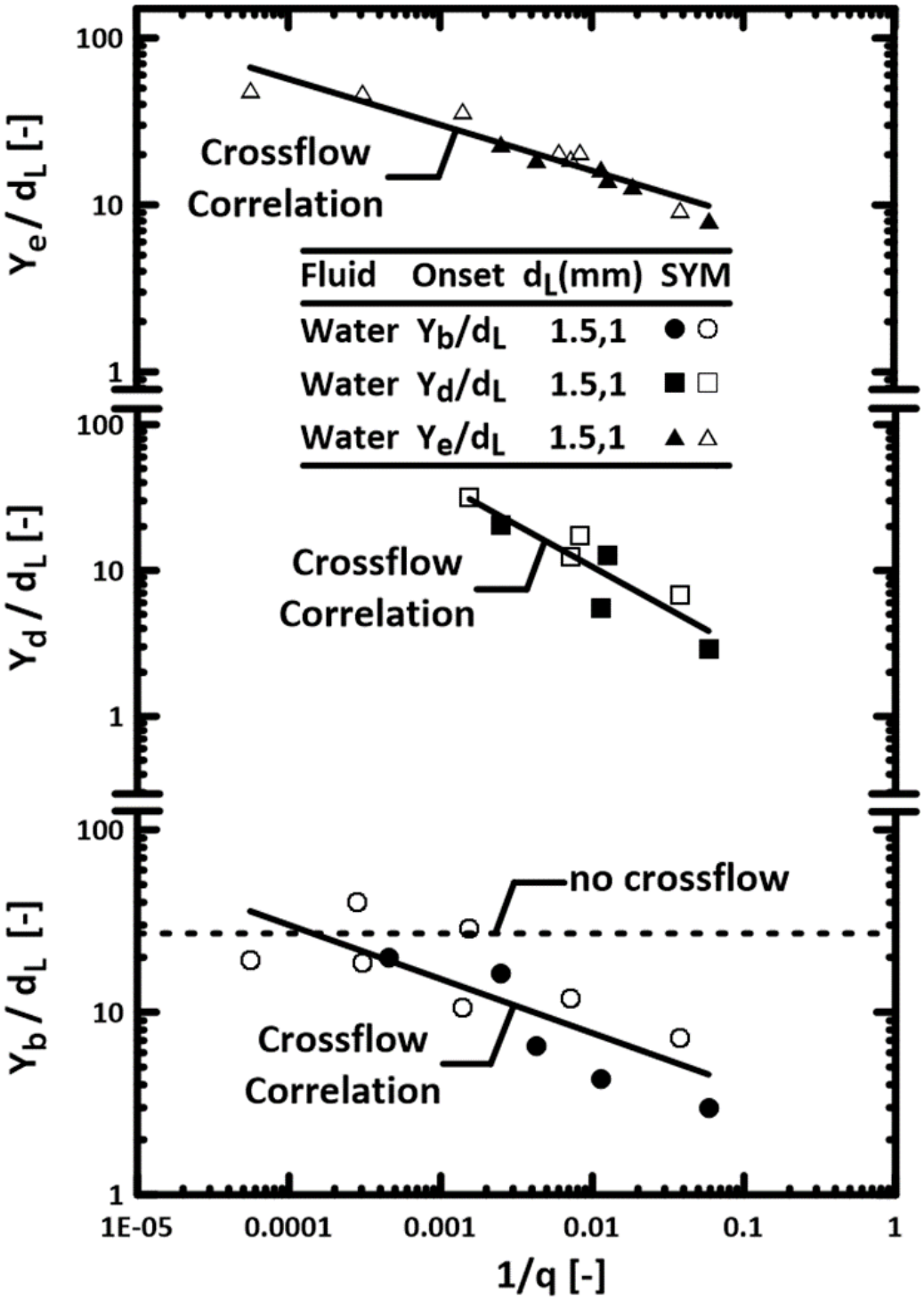

Figure 2.10. Onset of bag, drop and end of liquid core for fan nozzles (d_L = 1.5 mm and 1 mm) vs 1/q as non-crossflow regime is approached.

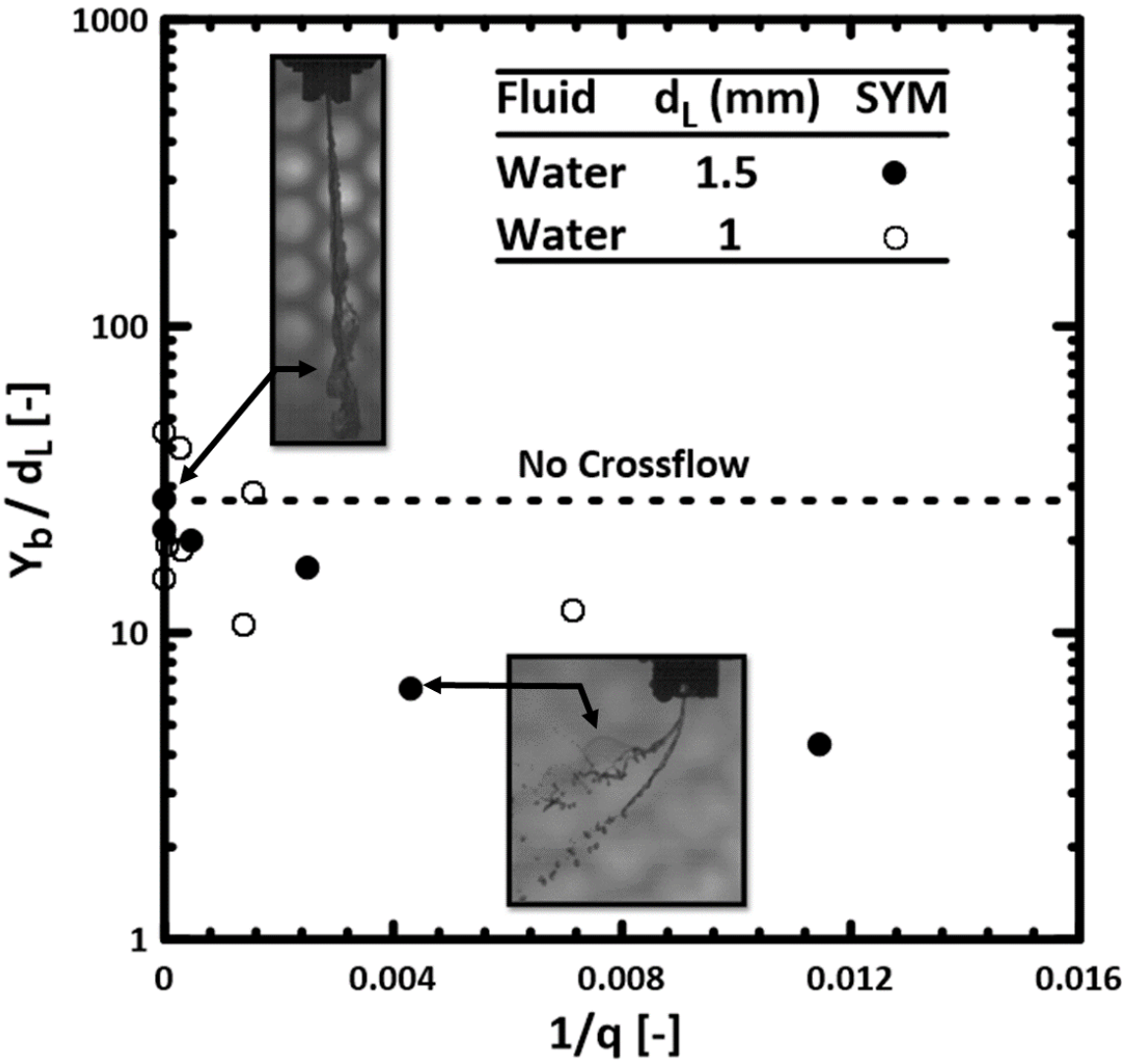

Figure 2.11. Onset of bag for fan nozzles (d_L = 1.5 mm and 1 mm) vs 1/q approaching the average onset of bags for the non-crossflow test conditions.

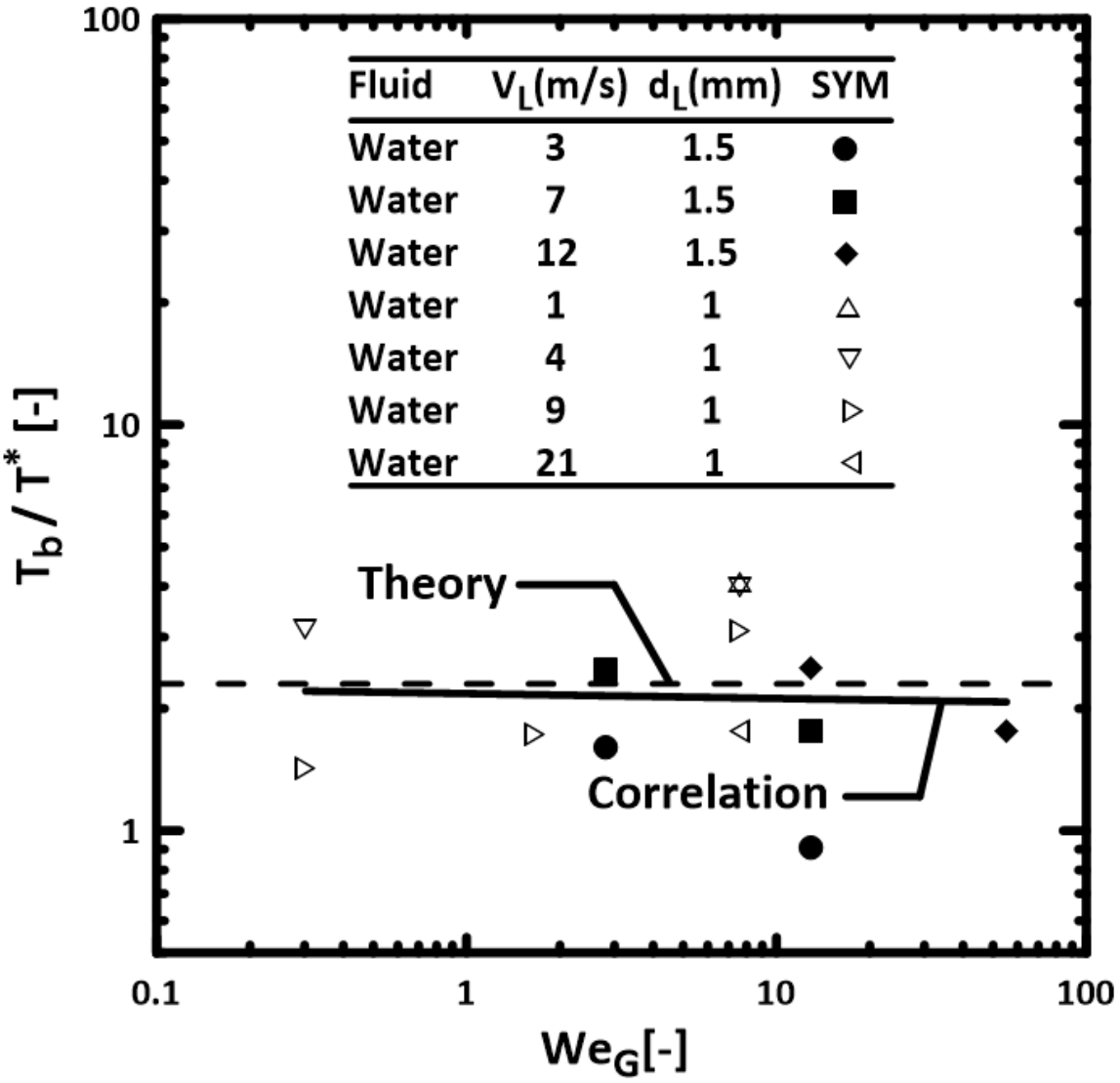

Figure 2.12. Dimensionless time of breakup based on regime (sheet, and bags) for 1.5 mm and 1 mm diameter nozzles.

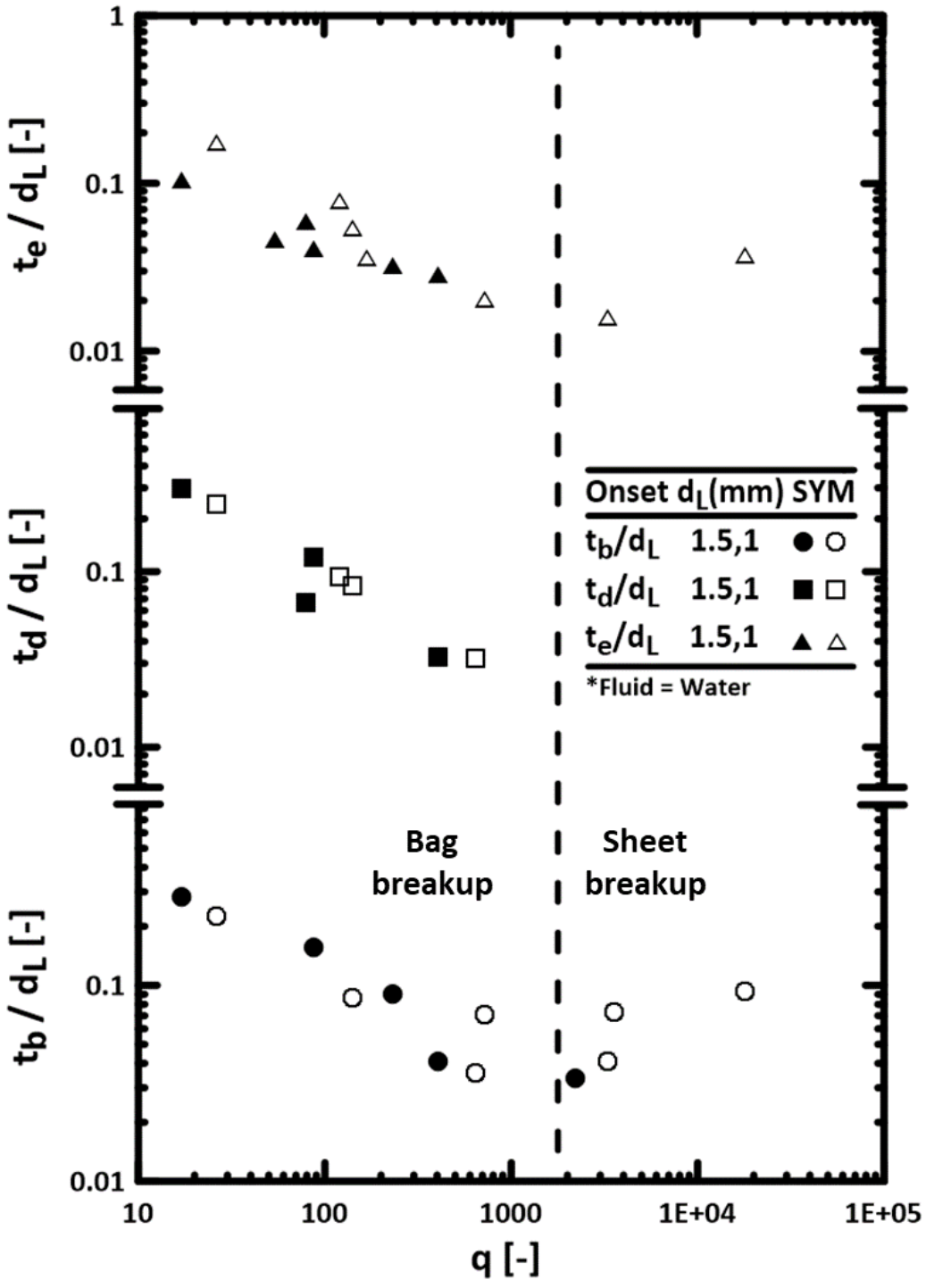

Figure 2.13. Dimensionless thickness as a function of q (momentum flux ratio) based on regime (sheet, and bags).

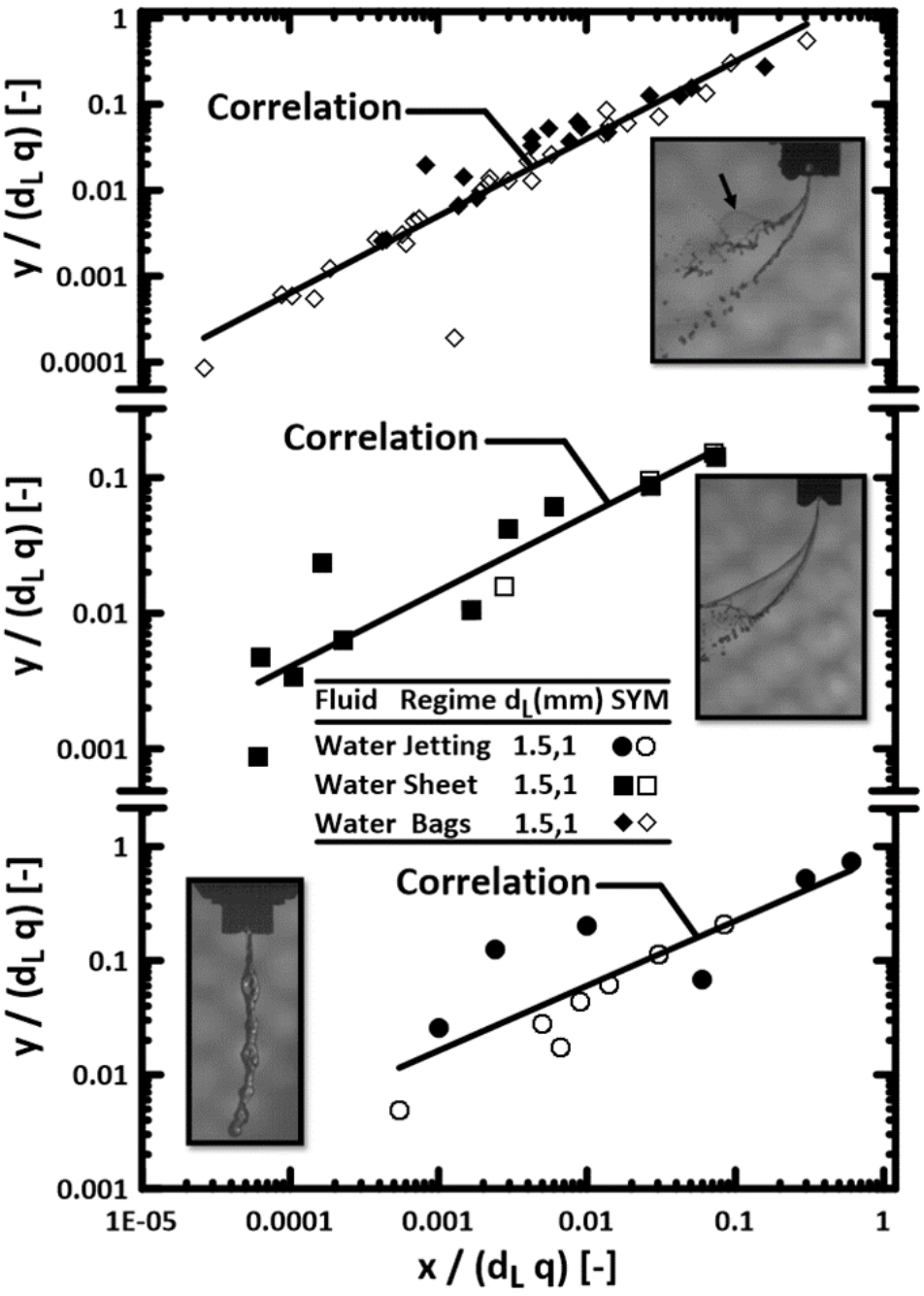

Figure 2.14. Dimensionless jet trajectory based on regime (jetting, sheet, and bags).

CHAPTER III

PRIMARY BREAKUP OF LIQUID JETS IN GASEOUS COFLOW

3.1. Introduction

Air assisted atomizers have widespread applications including the atomization of biomedical suspensions, production of powdered substances using spray freezing with applications in the food industry (Tanner et al., 2006), aerosols, combustion, painting and especially in high-speed air breathing propulsion (e.g., scramjet engines) due to their abilities to produce large penetration and smaller droplets from relatively large injector diameter among others. This atomization technique has been extensively studied using numerical simulations (Funada et al., 2006, Eggers & Villermaux, 2008, Kozul et al. 2020) and experimental approaches (Glathe et al., 2001, Ahmed et al., 2020, Murugan et al. 2020). It could successfully be combined with other atomization techniques. Ahmed et al. (2020) reported a new design of a hybrid air-blast and electrostatic atomizer that can be useful for the atomization of highly viscous fuels like biodiesel and demonstrated that droplet and ligament size are reduced with increasing of spray charge, with the maximum effect of the charge being found for the lowest Weber number.

Funada et al. (2006) provided a comprehensive theoretical model of temporal instability of a circular liquid jet in a coflowing high speed air stream using viscous potential flow. The model predicts that with the increase in air stream speed there is a reduction of breakup fragments of liquid (Funada et al., 2006).

Zhang et al. (2021) has developed a model for air-assisted atomization of high-viscous glycerol/water jet injected into a coaxial airflow where the atomization occurs at elevated ambient pressures and found out that high pressure results in shorter breakup length. Simulations also show that liquid has strong kinetic energy at higher pressures because of momentum transfer from gas to liquid phase (Zhang et al., 2020). Yang et al. (2020) developed a model for the explicit expression of Sauter Mean Diameter (SMD) which favorably matched the experimental data.

The geometry of the injector received considerable interest, e.g., Glathe et al. (2001) experimentally studied the effect of air assisted atomization of liquid in the setup where liquid was delivered through a central tube, and the air was delivered through the annular orifice on the outer radius of the liquid tube. The author demonstrated noticeable effects of eccentricity of the central tube (i.e., that changed the geometry of the air co-flow relative to the liquid stream) on the air-assisted atomization using high speed airflow (Glathe et al., 2001). A study by Kumar and Sahu (2018) found substantial contribution of the liquid-centered coaxial injector's exit geometry on liquid jet breakup in a high-speed annular air stream. By employing a swirl air blast atomizer design, Soni and Kolhe (2021) demonstrated that the use of annular swirl air can effectively reduce the jet breakup length and contribute to better air-fuel mixing and vaporization characteristics. Watanawanyoo et al. (2011) developed a twin fluid atomizer for fuel injection to study the droplet characteristics using shadowgraphy technique. Various sized droplets and droplet distribution were observed by keeping the liquid pressure constant and varying air flow rate.

According to findings by Marmottant and Villermaux (2004), an air-assisted atomization is initialized by a Kelvin–Helmholtz instability which generates interfacial waves on the liquid core by aerodynamic forces. This first stage is followed by the surface perturbations due to the Rayleigh–Taylor instability, where liquid structures protruding from the liquid surface are accelerated by aerodynamic interactions, leading to disintegration of the intact jet core. The above

two-stages process is referred to as primary atomization which, in cases where droplets exceed a critical size, is followed by secondary atomization to form smaller droplets. According to Yang et al. (2020) the liquid jet is first subjected to the Kelvin–Helmholtz instability which forms a liquid ligament followed by airflow assisted breakup of the filament into fine droplets through the effects of Rayleigh–Taylor instability. Kumar and Sahu (2018) investigated the unsteady behavior of the liquid jet breakup under the effects of coflowing air stream and reported the formation of Kevin-Helmholtz instability one diameter from the jet and flapping instabilities were observed further downstream of the jet due to weak effects of the Momentum flux ratio as Reynolds number dominates the downstream region of the jet. Lasheras et al. (1997) studied the breakup and atomization outcomes of a round liquid jet operated under the influence of high-speed annular gas jet using Phase Doppler particle (PDP) and flow visualizations, the primary breakup was attributed to the disturbances introduced into the flow that results in fragments followed by secondary breakup where the fragments are further atomized into finer droplets. The author further reported two effects due to the transport of large-scale structures which are the main reason for the spreading of jet; one is the increasing droplet size as the distance from the jet increases and the other is to entrain the surrounding air into the spray region which is comparable to the radius of the spray.

Khan et al. (2019) tested twin fluid atomizers at ultra-low flow rates and demonstrated that air velocity is the main factor, controlling the atomization process in flow blurring injectors and furthermore showed that ALR (Air-liquid ratio) decreases as a function of LFR. (Liquid flow rate). Barreras et al. successfully tested two different nozzle geometries and found out that nozzle geometry does not affect the ALR, however an increase in Cd is observed with different geometries. An equation that relates drop size to the air Reynolds number has also been developed (Barreras et al., 2006). Leroux et al. (2007) used fast Shadowgraphy technique to study coaxial atomizers by varying liquid properties (viscosity, surface tension) and nozzle geometry.

Momentum flux and Reynolds number play a key role in characterizing the spray and jet disintegration. The primary atomization process in coaxial injectors was mainly ruled by aerodynamic effects. Hardalupas and Whitelaw (1994) studied coaxial air blast atomizers and found out that at same gas to liquid velocity ratios, the atomization outcomes improve with smaller liquid tube diameter resulting in reduced spray width. He further quantified that the presence of a converging nozzle at gas jet exit enhances the atomization and increases spray spread rate for low gas-liquid velocity ratios.

Wachter et al. (2021) investigated the effects of gas gap width, pressure, and gas velocity on Sauter mean Diameter and developed an empirical model for pressure scaling in twin fluid atomizers based on momentum flow ratio. The droplets decreased with increasing pressure and gas gap width. However, increasing gas velocity results in increasing droplet diameter. Varga et al. (2003) used two different nozzle geometries to investigate the initial breakup of small diameter liquid jet operated under high velocity gaseous stream (air) with 10 times the diameter of the liquid jet using PDA. He reported the effects of viscosity on the SMD by using two fluids ethanol and water and it was observed that in all the cases the SMD for ethanol was smaller. A new Weber number based on the wavelength of liquid was developed to explain the primary breakup process which was initiated as a result of R-T instability also referred to as the primary mechanism for initial breakup whereas KHI was reported to be dominant in the secondary breakup.

Wachter et al. (2020) investigated the effects of gas jet angle on the droplet sizes and primary breakup in coaxial twin fluid atomizer configuration it was found that, higher gas jet angle results in higher radial component which destabilizes the jet earlier. The author also reported that higher momentum flux ratio is required with increasing gas jet angle to form Kevin Helmholtz as the KHI develop within the intact liquid core. Liu et al. (2005) investigated coaxial atomizer and reported that high momentum flux ratio flows had a greater effect on the Sauter Mean Diameter;

however, no effect was triggered with small values of momentum flux ratio. They further developed an expression for calculating SMD based on liquid/gas velocities, diameter, and momentum flux ratio.

Wu and Faeth (1995) investigated turbulent liquid jets in still air at different Weber numbers and found out an expression for onset of surface breakup, end of surface breakup and length of the intact liquid core. He further characterized the breakup based on We number, 1st induced was observed at lower We are showing only onset of surface breakup, increasing the We further results in both onset and end surface breaks and then finally with higher We 2^{nd} wind induced is observed and surface breakup is seen even after the liquid column. Tian et al. (2014) investigated the behavior of liquid entrainment process near the exit of the atomizer. The formation of a liquid bulge because of increased gas velocity was observed that travels upwards filling the central tube with liquid at higher gas velocities, and it was found that liquid velocity has a linear relation with the critical gas velocity for all atomizers. The entrainment was further characterized as initial and full entrainment. Small diameter nozzles have higher values of critical velocities compared to larger diameter nozzles due to the weakening of shear force with increasing diameter. Porcheron et al. (2002) investigated the effects of gas injection density on the primary breakup of liquid jet. It was observed that at fixed momentum flux ratio and liquid velocity, the axial velocity of the gas decreases much faster at low density compared to high density gases that atomize the jet more efficiently.

In recent studies micro injectors have been used, however no study shows the effect of very low Weber number. Levy et al. (2006) investigated two miniature air-assisted (small swirl and air assist) atomizers using PDPA, the results showed a decrease in SMD because of increases pressure drop and the velocity being shifted to the periphery away from the center in swirl atomizer, however maximum droplet velocity is observed at the center for air- assisted atomizers. Higher velocity at higher liquid pressures has slight effects on the drop size, at a liquid pressure

of more than 4 bars a constant angel of 90 degrees has also been observed by the author. Wang et al. (2006) studied two twin fluid atomizers. The study showed that breakup process due to instabilities and oscillation is directly related to the atomization mechanism. It was also shown that the droplet size decreased significantly at lower GLR (Gas-liquid ratio), hence proving that the atomization process in micro twin fluid atomizers is mainly dominated by surface tension.

Most of these studies, however, were limited to relatively large injectors and weber numbers. Of interest in the present study is the impact of shrinking injector size and small weber number on the breakup outcomes. The objective of this paper is to investigate the breakup outcomes of a beveled micro needle, used to inject test liquid into a coflowing airstream injected from a larger beveled needle motivated by the potential usage as disposable and inexpensive atomizers in variety of medical and industrial applications.

3.2 Experimental Methods:

The present coflowing atomizer is assembled from two beveled needles (16G and 30G one inside the other, with the smaller needle resting against the inner wall of the larger needle, as shown in Fig. 3.1 The needles are supported by a mount to avoid shaking of the system due to high pressure. An adjustable tuner is used to align the needle with the laser sheet and the camera. The pressure of city water line (50 psig) was used to feed the test liquid (water). Shop air (maximum 110 psig) air was used to generate the coflowing air in the outer needle, as shown in Fig. 3.1. Two inline filters capable of filtering up to 40 microns (not shown in Fig. 3.2) are used to clean the water before delivering it to the needle to avoid blockages. Two different Rotameters (Omega Engineering & Dakota Instruments) are used to measure the flow rate of air and water that is supplied to the atomizer. The diagnostics consists of double-pulsed shadowgraphy. Two Nd: YAG lasers (New wave laser, 70 mJ/pulse, 10 Hz) generated the laser beams. The two beams were aligned, expanded, and collimated as shown in Fig. 3.2. A diffusing screen was used to

provide the background illumination. A double exposure camera (pco.2000, 2048 x 2048 pixel) with 60 mm Nikkor lens was used to record the image. A delay generator is used to time the two laser pulses and the camera exposures. Two images are taken with the desired pulse separation for velocity measurements. An oscilloscope is used to measure the pulse separation. The test conditions include 5 different air flow rates. At each air flow rate five different water flow rates are tested to study the effects of air on the atomizer behavior. The Rotameter was calibrated with the conventional flow rate measurement method of bucket and stopwatch to make sure it matches with the calibration chart provided by the manufacturer and to avoid any errors in measurements. The data points were then fitted with a power equation to calculate the volumetric flowrates that were not listed in the calibration chart. Mass flow rates for both the air and the water were calculated using the following equations:

$$\dot{m}_L = \rho_L Q_L \tag{3.1}$$

$$\dot{m}_G = \rho_G Q_G \tag{3.2}$$

A calibration image was taken by focusing on the standard chart used in air force, which can help determine the resolution of the images that can be acquired with the current magnification of the camera, and to serve for measurement purposes.

ImageJ software was used to analyze the images and all the measurements were restricted to within 10% of the statistical uncertainty of 95% confidence interval. The liquid jet velocity was calculated by dividing the liquid volumetric flow rate by the internal cross section area of the inner needle. The gas (air) velocity was calculated by dividing the volumetric flow rate of the air flow, as measured by the rotameter, by the cross-section area of the annular flow between the outer and inner needles. The liquid velocity ranged from 0.25 - 0.5 m/s while the gas velocity ranged from 32 -151 m/s, the test conditions are summarized in (Table. 3.1). The results include droplet diameter at onset, intact breakup length and time of breakup.

3.3. Results and Discussion:

The experiment was performed by using only the inner needle with liquid as the working fluid. The results show beveled needle injector behave like cylindrical injector with Rayleigh breakup at low flow rates. In the absence of coflow, the breakup length increases as a function of liquid flow rate, then decreases as the jet velocity increases and the surface tension becomes weaker, and at higher jet velocities the breakup length increases as the jet remains intact for a longer time before it breaks, however this trend needs to be proven by testing the liquid jet at higher flow rates. A graph is plotted as shown in Fig. 3.3 to show the above-described trend of the dimensionless breakup length of the liquid jet as a function of the liquid weber number We_L. The current study was limited to very small weber numbers, the closest comparison that could be found was the study of Rajendran et al. (2012), that shows an increasing trend for various liquids and different diameters and this data agrees well with the study of Grant and Middleman (1966) for a round liquid jet in still air.

The effect of coflowing air was investigated by varying the flow rate as shown in Fig. 3.4, as the air velocity increases from left to right a decrease in the breakup length is seen due to the dominating effect of the aerodynamic forces. Flow visualization in Fig. 3.5 shows the effect of increasing jet velocity resulting in longer breakup length because of stronger surface tension forces overcoming the weak inertial forces and hence remain intact further downstream.

The air and liquid flow rates are controlled independently in the present setup, using two separate Rotameters. The air velocity does not affect the liquid flow rate, as shown in Fig. 3.6. This allowed flexibility in setting up the test matrix. This also allowed to confirm if there were leaks that could affect the flow rate of the jet.

The breakup length of the liquid jet (defined as the length of the intact core length) is controlled by controlling the flowrate of both liquid and air flowrates, as shown in Fig. 3.7. The breakup

length increases initially due to stronger surface tension that keeps the liquid intact for a longer length until air forces weaken the jet stream, as the air velocity increases the breakup length tends to decrease due to stronger air effects that weakens the surface tension among the liquid molecules and hence the breakup happens earlier. The dimensionless breakup length was plotted as a function of gas-liquid momentum ratio (1/q) as shown in Fig. 3.7 to illustrate the effects of increasing velocity on the breakup length and it is clearly seen that breakup length increases as a function of increasing 1/q (which means higher gas velocity). A correlation has been obtained with a correlation coefficient of R = 0.96 as follows:

$$L_c/d_L = 42\ (1/q)^{-0.26} \tag{3.3}$$

The current correlation is compared with the correlation of Leroux et al. (2007) in Fig. 3.7 for d_L = 1 mm, and is given by:

$$L_c/d_L = 10\ (1/q)^{-0.3} \tag{3.4}$$

The breakup length shows the same trend however it breaks much earlier compared to the present study this can be attributed to the fact that the current atomizers is order of magnitude smaller than the atomizer used in Leroux et al. study, to further understand if this phenomenon is valid the data from Kumar and Sahu (2018), with d_L = 3 mm, was also compared in Fig. 3.7. It was found that the breakup length was smaller than both Leroux et al. (2007) and present study for d_L= 0.1 mm. This suggests that the nozzle diameter has a strong effect on the breakup length.

The time of breakup has also been investigated and given as:

$$T_b/T_R \tag{3.5}$$

Where Tb is the time required for the breakup and T_R is the Rayleigh breakup time. T_R is used as the current study was limited to very small liquid flow rates. The time of breakup starts in the Rayleigh regime and as the coflow Weber number increases the aerodynamic effects become

dominant which destabilizes the jet and hence it takes less time to break the jet (Fig. 3.8). The correlation for the time of breakup is obtained as follows with the correlation coefficient R = 0.96:

$$T_b/T_R = We_{GL}^{-0.7} \quad (3.6)$$

The droplet sizes at onset were measured and plotted as function of the gas-liquid weber number We_{GL}, as shown in Fig. 3.9. Similar to the time of breakup the droplets start in the Rayleigh regime with droplet size twice the size of the jet diameter, as the aerodynamic effects become prominent due to the increase in air velocity the droplet sizes are reduced. The higher air velocity tends to shear the liquid core, reduces the breakup length and producing smaller droplets. The following correlation for the drop sizes has been obtained with a correlation coefficient R = 0.85:

$$d_i/d_L = 2.4\ We_{GL}^{-0.2} \quad (3.7)$$

Of interest is the spatial distribution of spray and the effects of secondary breakup. Due to the high magnification of the present setup the depth of focus was small. This became problematic as the measuring volume is moved downstream and very few droplets are in focus with many droplets out of focus due to the three-dimensional nature of the spray. To measure the droplet sizes as function of distance from the jet exit it is crucial to use three-dimensional imaging technique. Therefore, the next step is to use digital holography. Additionally, the air velocity currently is calculated assuming constant density between the rotameter and the needle exit. This will be corrected in future work. The research team plan to generate a breakup regime map and to investigate the spray size distribution as a function of the distance from the injector exit, and large data set of drop sizes and drop velocities.

3.4. Conclusions:

The major conclusions for the study the breakup of coflow liquid jet are as follows:

1. At small Weber number, We_{GL}, the breakup time is similar to Rayleigh breakup time of a laminar liquid jet, indicating negligible effect of the nozzle geometry and coflow. At high Weber number there is a decreasing trend that indicate a stronger aerodynamic effect.
2. The droplets sizes produced at lower Weber number are bigger than the jet diameter (twice) typical of Rayleigh breakup for a laminar liquid jet.
3. The breakup length is a strong function of the momentum flux ratio (q).

Table. 3.1 Test conditions for coflow experiment

Parameters	Value
Liquid density, ρ_L [kg/m^3]	997
Gas density, ρ_G [kg/m^3]	1.23
Surface tension, σ [N/m]	0.072
Jet exit diameter, d_L [mm]	0.16
Gas-Liquid momentum ratio, 1/q [-]	20 - 100
Liquid Weber number, We_L [-]	0.1 - 0.6
Gas-Liquid Weber number, We_{GL} [-]	2.7 – 62
Gas Velocity, V_G [m/s]	32 - 151
Liquid Velocity, V_L [m/s]	0.25 - 0.5

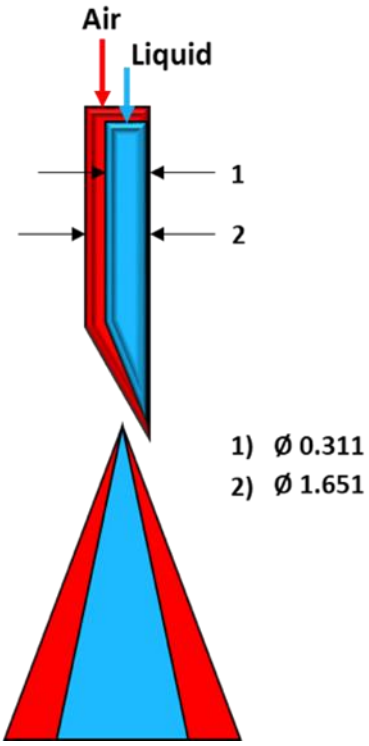

Fig. 3.1 Sketch of the present coflow injector.

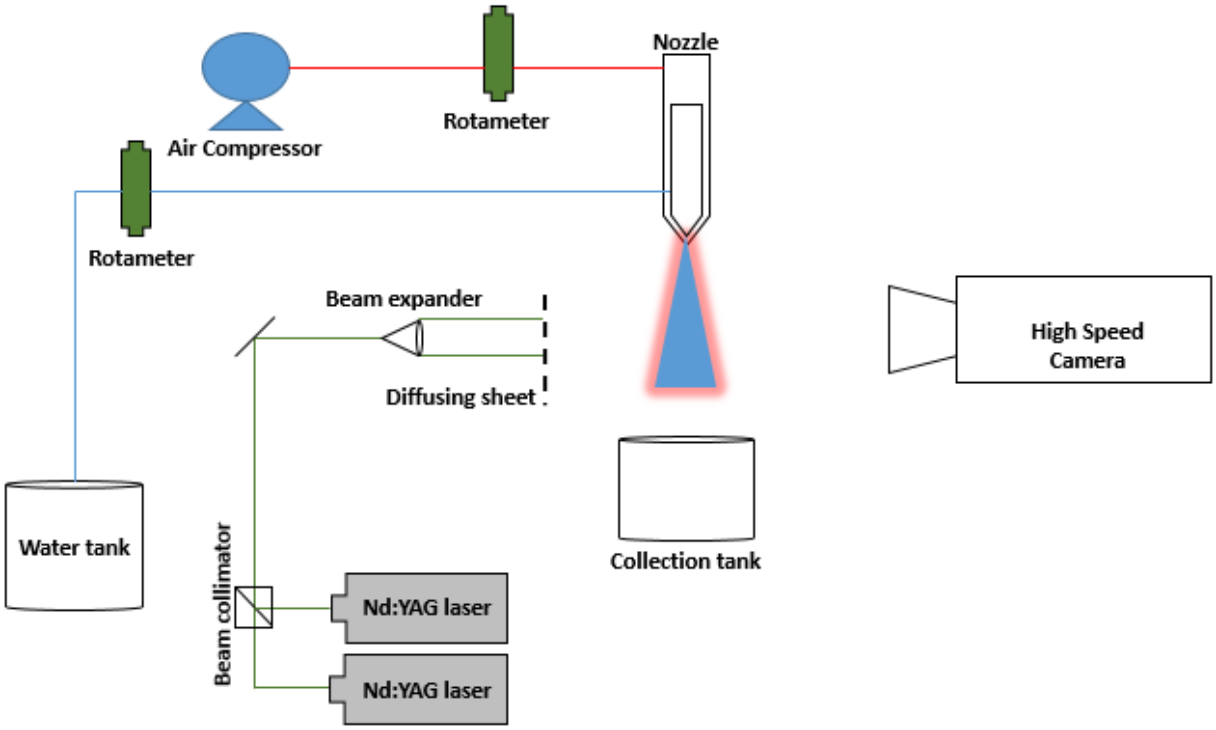

Fig. 3.2 Sketch of the apparatus for coflow experiment.

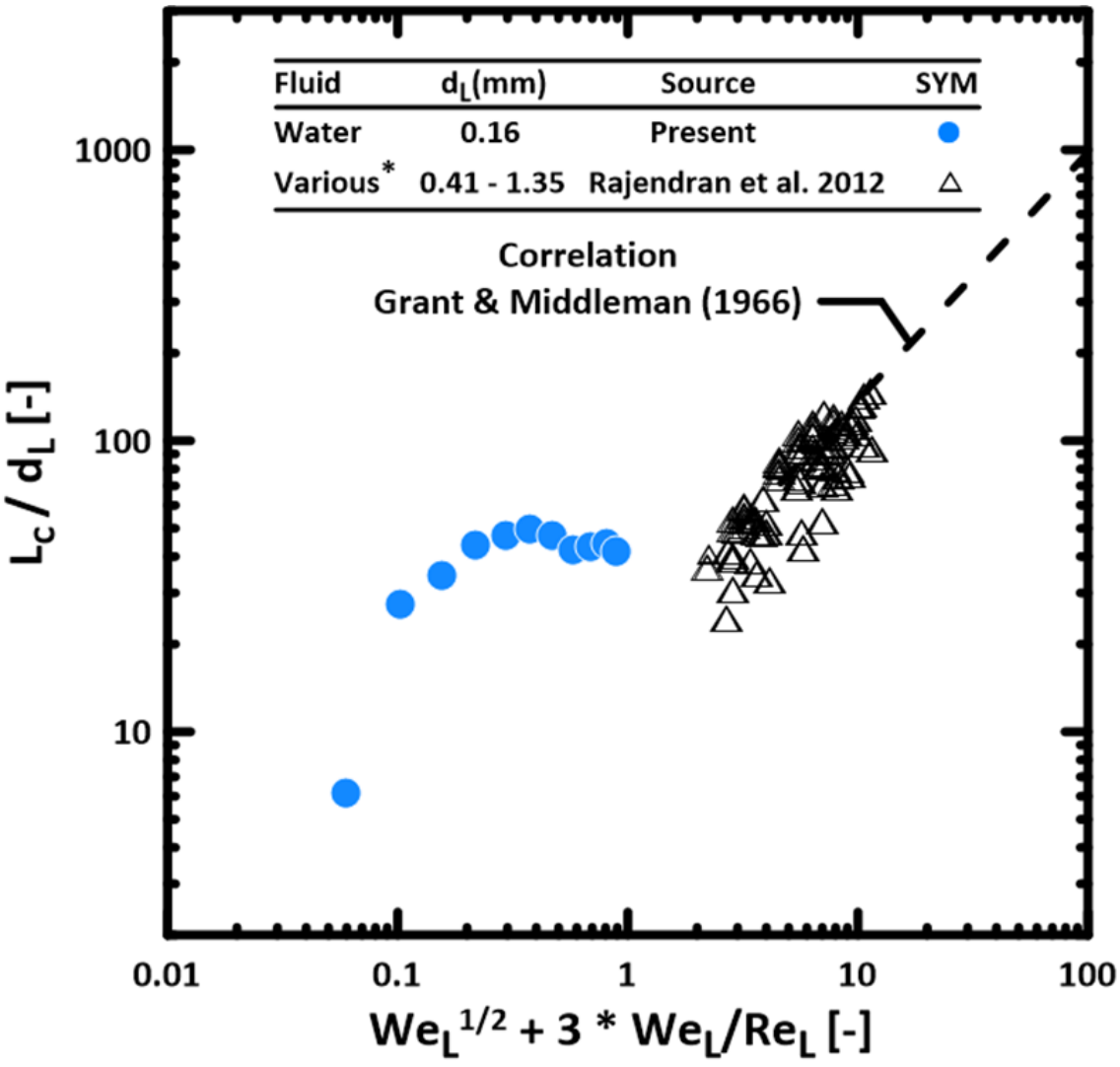

Fig. 3.3 Dimensionless breakup length as a function of liquid Weber number, plotted together with previous studies.

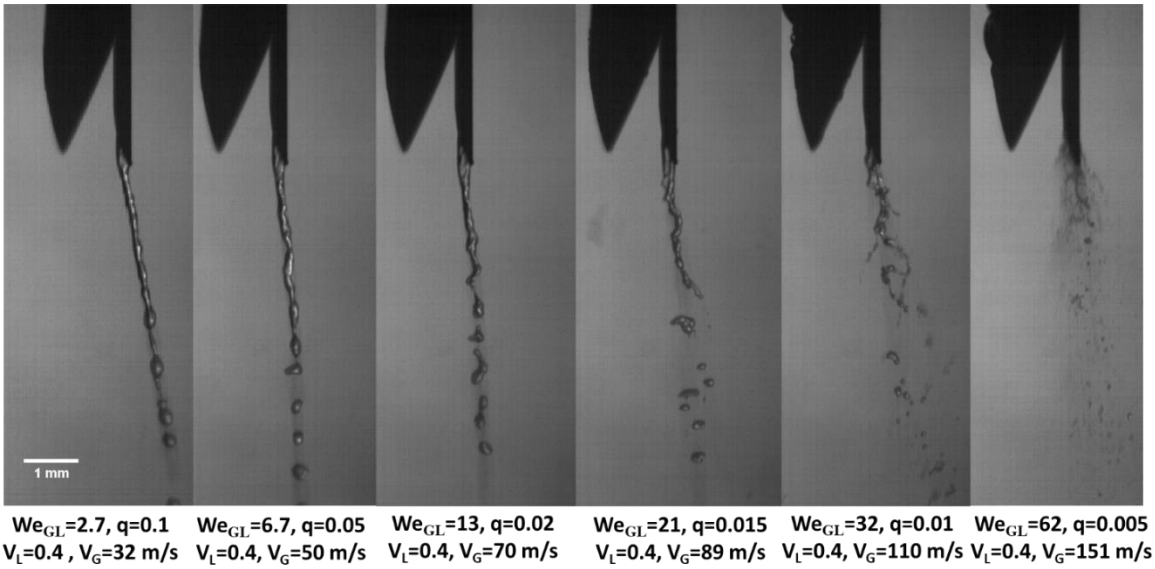

Fig. 3.4 The effect of air flow rate on a constant jet velocity of 0.4 m/s.

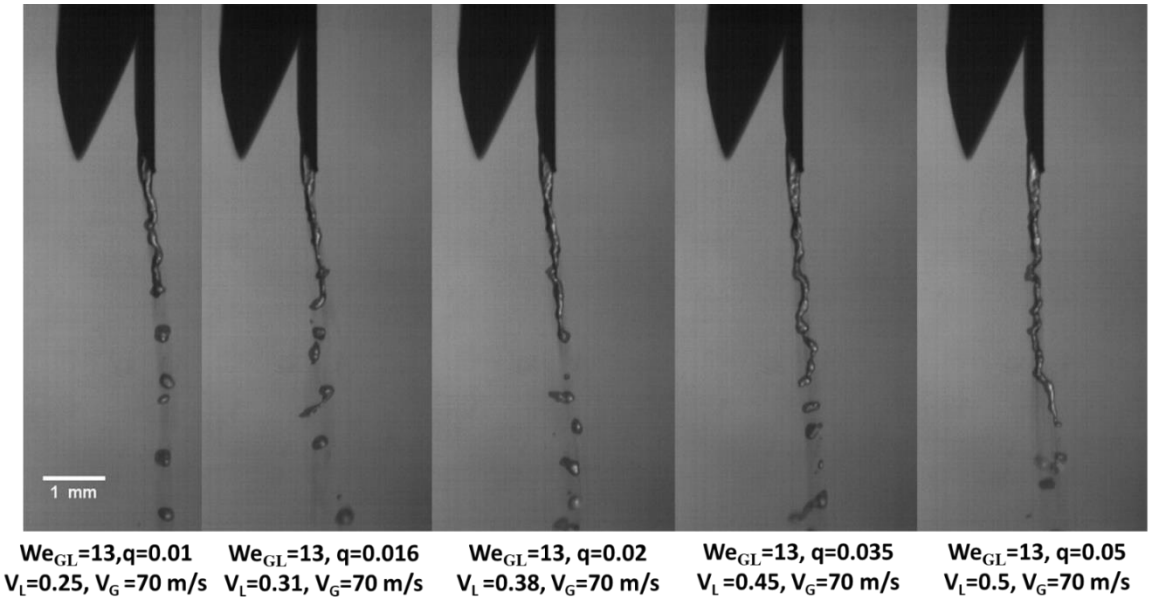

Fig. 3.5 The effect of varying liquid jet velocity at a constant air velocity of 70 m/s.

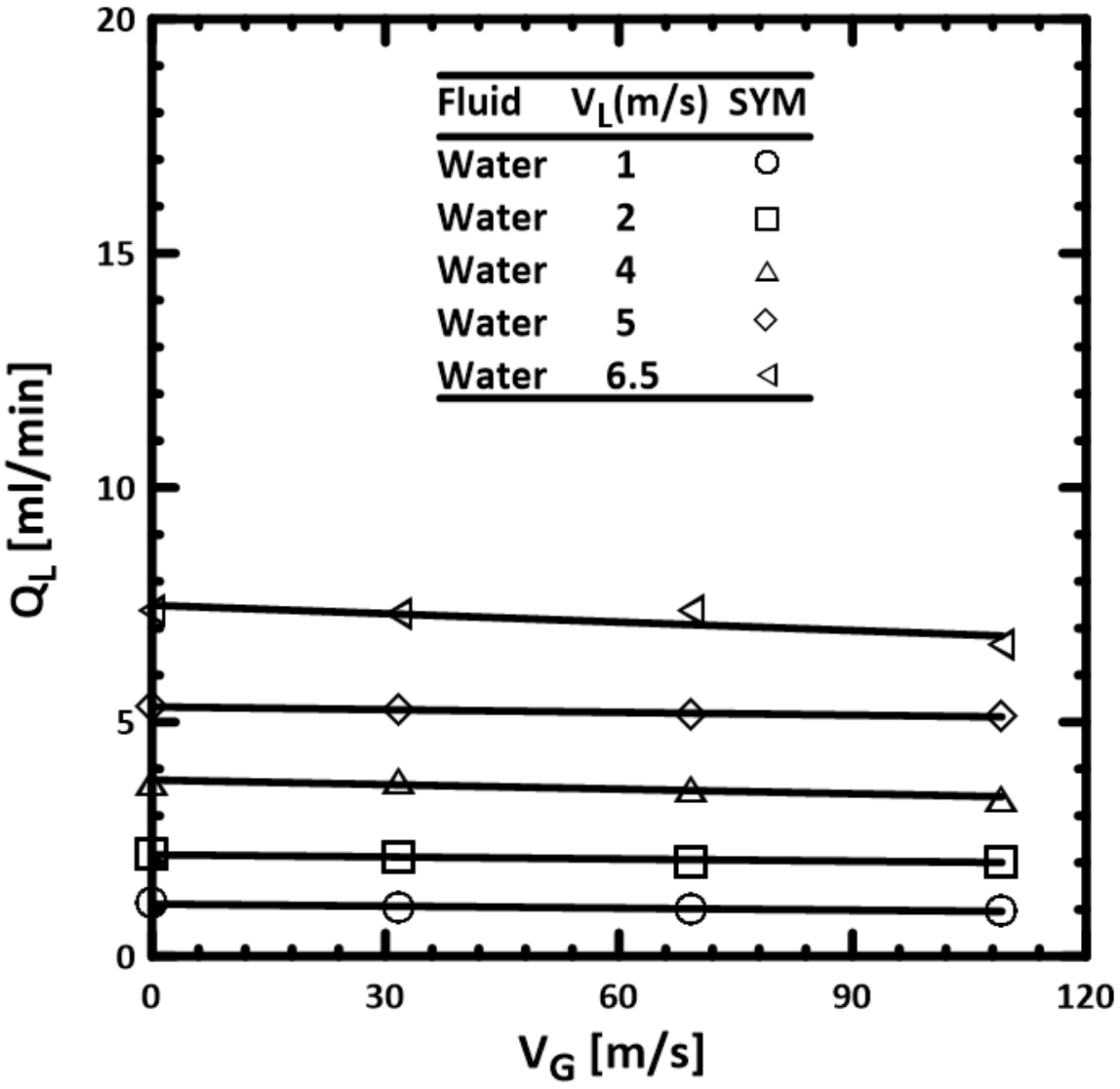

Fig. 3.6 Liquid flow rate as a function of Air Velocity, tested at 5 different water flow rates and three different air velocities.

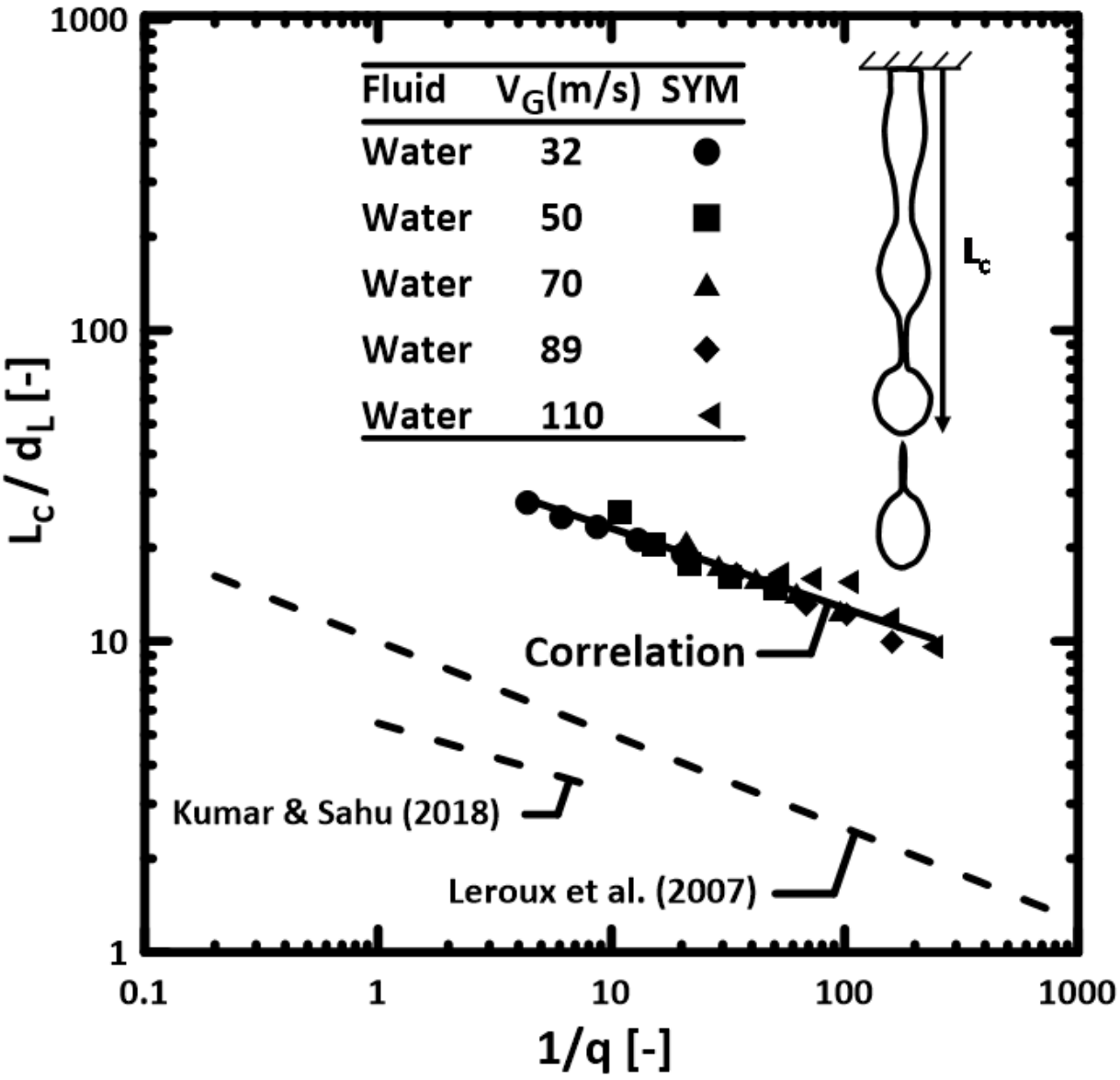

Fig. 3.7 Dimensionless breakup length as a function of momentum flux ratio (1/q).

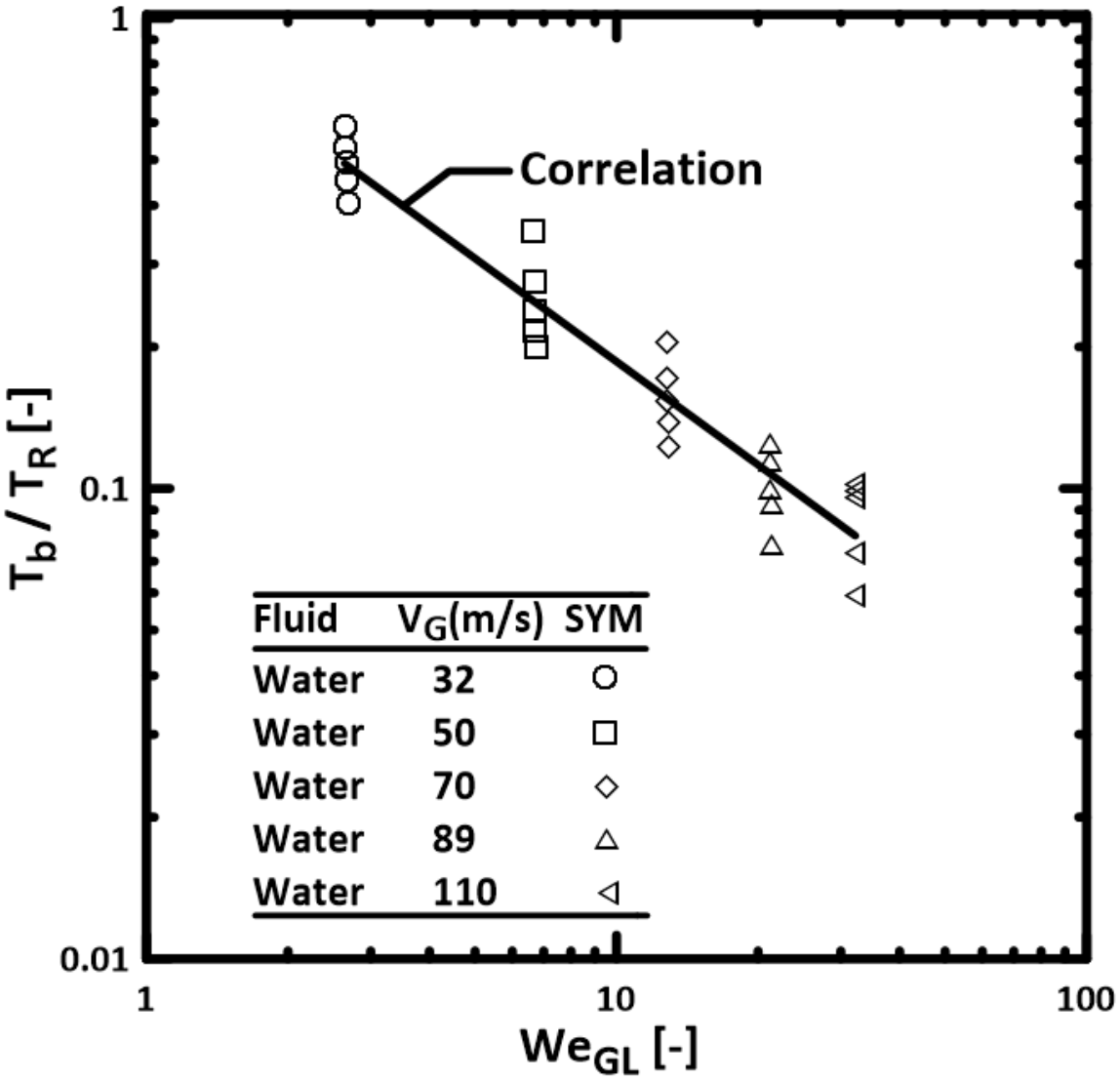

Fig. 3.8 Rayleigh time of breakup vs gaseous Weber number.

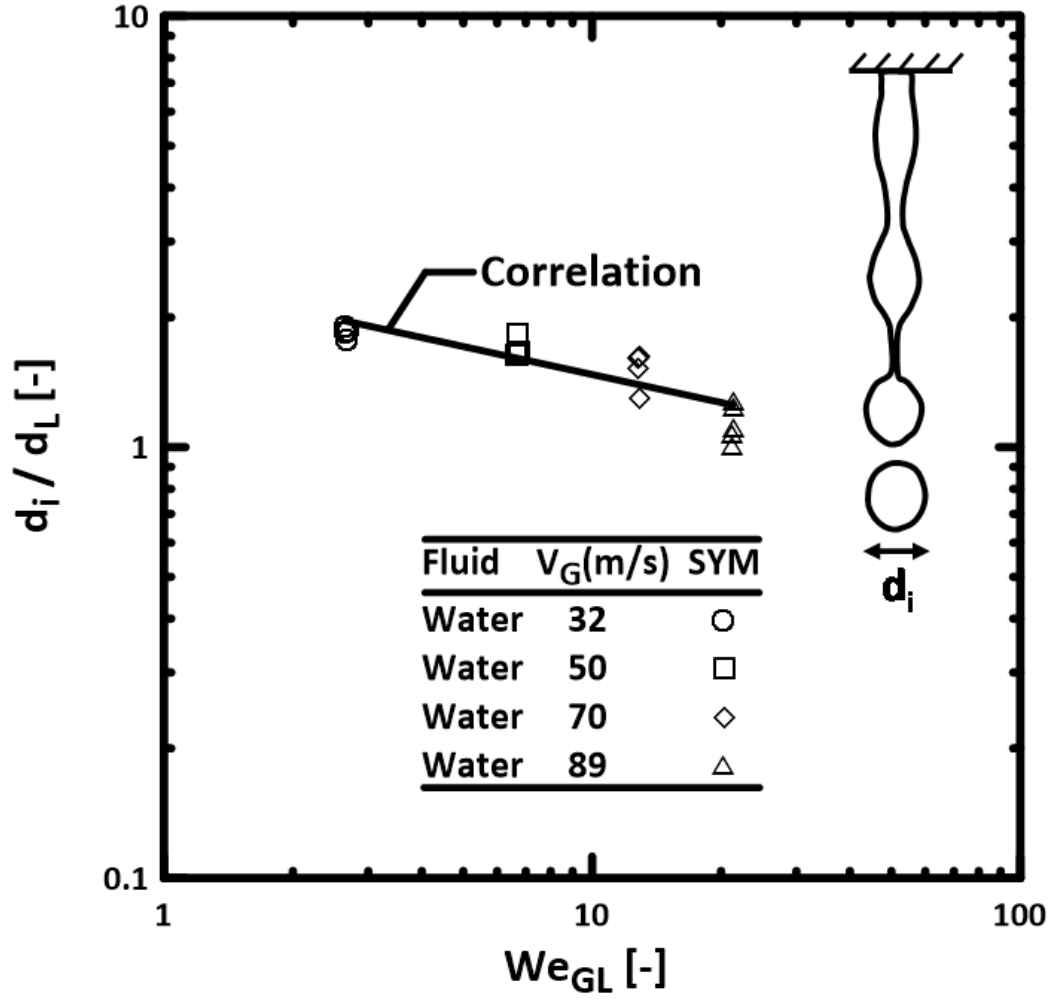

Fig. 3.9 Droplet diameter as a function gas-liquid Weber number.

CHAPTER IV

SUMMARY, CONCLUSIONS, AND RECOMMENDATIONS

4.1 SUMMARY:

The aerodynamic effects on primary breakup were studied for two injection configuration, liquid sheet from flat fan nozzle injected in crossflow and round liquid jet injected from beveled nozzle in coflow. The breakup of flat fan nozzle spray in crosswind was investigated experimentally motivated by its application to the agricultural sprays, and specifically the drift of some herbicides that can cause serious damage to genetically unmodified crops. Instrumentation consists of high-speed imaging. The test conditions included We_L ranging from 13-14486 and the We_G ranging from 0.3 – 55 to simulate the aerodynamic effects on the liquid sheet breakup in different windy conditions. The measurements include the breakup regime transitions, onset of breakup including onset of bags, onset of drop, the location of the end of the intact liquid core, the breakup time, and the liquid core trajectory.

The air-assisted atomization of a micro liquid jet injected from beveled needle point style injector in coflow was studied experimentally motivated by its potential applications in biomedical spraying applications. The primary breakup mechanism is investigated using high speed imaging. The test conditions included We_L ranging from 0.14 – 0.6 and the We_{GL} ranging from 2.7 - 62. The results included the intact core length, the location of the onset of liquid jet breakup, size of drops at onset and time of breakup. The results are interpreted using phenomenological analysis.

4.2 CONCLUSIONS:

The major conclusions for the study the breakup characteristics of liquid sheet injected from flat fan nozzles in crossflow wind are as follows:

1. The fan angle of the liquid sheet is controlled by the liquid flow rate at low flow rate before reaching its rated fan angle at the rated flowrate.
2. The crossflow can change the primary breakup mechanism from sheet breakup regime to bag breakup regime. Those bag structures break into smaller drop sizes than the drops resulting from the sheet breakup which results in an increased spray drift flux in crosswind. The breakup regime transition from sheet to bag breakup is triggered when the momentum flux ratio, q, becomes smaller than 200.
3. Flapping bag breakup was observed at higher liquid flow rates due to surface instability. Those bags, observed previously at no crossflow condition, do not get stretched large enough to dominate the breakup mechanism of the liquid sheet.
4. The dimensionless breakup time for sheet and bag breakup is independent of the nozzle diameter and crossflow Weber number.

The major conclusions for the study the breakup of coflow liquid jet are as follows:

5. At small Weber number, We_{GL}, the breakup time is similar to Rayleigh breakup time of a laminar liquid jet, indicating negligible effect of the nozzle geometry and coflow. At high Weber number there is a decreasing trend that indicate a stronger aerodynamic effect.
6. The droplets sizes produced at lower Weber number are bigger than the jet diameter (twice) typical of Rayleigh breakup for a laminar liquid jet.
7. The breakup length is a strong function of the momentum flux ratio (q).

4.3 RECOMMENDATIONS:

The recommendations for future studies of the breakup of liquid sheet in crossflow are as follows:

1. The current study was conducted with water as the test liquid. Adding adjuvants, similar to agricultural sprays, would affect the disturbances growth and hence impact the sheet breakup length which effects the outcome of the spray (Ellis, 2001). Therefore, in future studies different formulations that are typical to herbicides should be implemented to better understand the spraying behavior of herbicides and pesticides. Additionally, the behavior of more viscous fluids should be investigated to incorporate the effects of the viscous force (Ohnesorge number) on the breakup mechanism and atomization outcomes. The current results should be confirmed by expanding the test matrix to include several sizes of flat fan nozzles.
2. The present results were limited to breakup regime transitions and location of onset of breakup. Droplet sizes produced without crossflow and droplet sizes due to bag breakup were not measured due to limited field of view (FOV) in case of injection in still air and limited resolution in case of bag breakup in crossflow. Therefore, there is a need for a larger FOV and a higher resolution to be implemented in future studies. Future studies should focus on droplet size measurements before and after the onset of crosswind-induced bag breakup.
3. There is a need to quantify the breakup rate and the percentage of drift able flux which is important to understand the danger of spraying harmful chemicals in windy conditions. Moreover, future studies should redesign the nozzle geometry and the injection angle to compensate for the crosswind velocity to precisely deliver the herbicides to the target area and reduce the phenomena of spray drift.

The recommendations for future studies of the breakup of liquid sheet in coflow are as follows:

1. The present test conditions were limited to a smaller range of the liquid flowrates due to the limitation of the liquid injection pressure in the current setup. These conditions can be extended to understand the primary breakup at extended range of Weber numbers. Also, the nozzle geometry tested was limited to beveled nozzle and should be further extended using different sizes and nozzle tip geometry.
2. The droplets sizes produced at higher air velocities were smaller than what can be measured with the resolution and depth of focus of the current imaging setup. Extending the range of investigated Weber number requires an improved imaging technique such as holography.

REFERENCES

Aalburg, C., et al. “Primary Breakup of Round Turbulent Liquid Jets in Uniform Gaseous Crossflows.” *43rd AIAA Aerospace Sciences Meeting and Exhibit*, 2005, https://doi.org/10.2514/6.2005-734.

Ahmed, T., et al. “Atomization Behaviour of a Hybrid Air-Blast-Electrostatic Atomizer for Spray Combustion.” Fuel, vol. 288, 2021, p. 119716., https://doi.org/10.1016/j.fuel.2020.119716.

Altieri, A., et al. “Mechanisms, Experiment, and Theory of Liquid Sheet Breakup and Drop Size from Agricultural Nozzles.” *Atomization and Sprays*, vol. 24, no. 8, 2014, pp. 695–721., https://doi.org/10.1615/atomizspr.2014008779.

Barreras, F., et al. “Experimental Characterization of industrial Twin-Fluid atomizers.” Atomization and Sprays, vol. 16, no. 2, 1 June 2006, pp. 127–146., http://doi.org/10.1615/atomizspr.v16.i2.10.

Broumand, M., et al. “Spatio-Temporal Dynamics and Disintegration of a Fan Liquid Sheet.” *Physics of Fluids*, vol. 33, no. 11, 2021, p. 112109., https://doi.org/10.1063/5.0063049.

Bueno, M. R., et al. “Assessment of Spray Drift from Pesticide Applications in Soybean Crops.” Biosystems Engineering, vol. 154, 2017, pp. 35–45., https://doi.org/10.1016/j.biosystemseng.2016.10.017.

Clark, C. J., and N. Dombrowski. “On the Formation of Drops from the Rims of Fan Spray Sheets.” Journal of Aerosol Science, vol. 3, no. 3, 1972, pp. 173–183., https://doi.org/10.1016/0021-8502(72)90156-5.

Derksen, R. C. et al. “Determining the Influence of Spray Quality, Nozzle Type, Spray Volume, and Air-Assisted Application Strategies on Deposition of Pesticides in Soybean Canopy.” Transactions of the ASABE, vol. 51, no. 5, 2008, pp. 1529–1537., https://doi.org/10.13031/2013.25301.

Dexter, R. W. “The Effect of Fluid Properties on the Spray Quality from a Flat Fan Nozzle.” Pesticide Formulations and Application Systems, vol. 20, 2001, pp. 27–43 https://doi.org/10.1520/stp10432s.

Doll, D. A., et al. “Effect of Nozzle Type and Pressure on the Efficacy of Spray Applications of the Bioherbicidal Fungus Microsphaeropsis Amaranthi1.” *Weed Technology*, vol. 19, no. 4, 2005, pp. 918–923., https://doi.org/10.1614/wt-04-352r2.1.

Dombrowski, N., et al. “Some Aspects of Liquid Flow through Fan Spray Nozzles.” Chemical Engineering Science, vol. 12, no. 2, 1960, p. 152., https://doi.org/10.1016/0009-2509(60)87012-1.

Dukes, J., et al. “A comparison of two ultra-low-volume spray nozzle systems using a multiple swath scenario for the aerial application of fenthion against adult mosquitoes.” *Journal of the American Mosquito Control Association*, vol. 20, no. 1, 2004, pp. 36–44.

Egan, J. F., et al. “A Meta-Analysis on the Effects of 2,4-D and Dicamba Drift on Soybean and Cotton.” Weed Science, vol. 62, no. 1, 2014, pp. 193–206., https://doi.org/10.1614/ws-d-13-00025.1.

Eggers, J., and E. Villermaux. “Physics of Liquid Jets.” *Reports on Progress in Physics*, vol. 71, no. 3, 2008, p. 036601., https://doi.org/10.1088/0034-4885/71/3/036601.

Ellis, M. C. B., et al. “The Effect of Some Adjuvants on Sprays Produced by Agricultural Flat Fan Nozzles.” Crop Protection, vol. 16, no. 1, 1997, pp. 41–50., https://doi.org/10.1016/s0261-2194(96)00065-8.

Fraser, R. P., and N. Dombrowski. “A Photographic Investigation into the Disintegration of Liquid Sheets.” Philosophical Transactions of the Royal Society of London. Series A, Mathematical and Physical Sciences, vol. 247, no. 924, 1954, pp. 101–130., https://doi.org/10.1098/rsta.1954.0014.

Funada, T., et al. “Liquid Jet in a High Mach Number Air Stream.” International Journal of Multiphase Flow, vol. 32, no. 1, 2006, pp. 20–50., https://doi.org/10.1016/j.ijmultiphaseflow.2005.07.006.

Glathe, A., et al. “The Influence of Eccentricity on the Performance of a Coaxial Prefilming Air-Assist Atomizer.” *Atomization and Sprays*, vol. 11, no. 1, 2001, pp. 21–33., https://doi.org/10.1615/atomizspr.v11.i1.20.

Grant, R. P., and S. Middleman. “Newtonian Jet Stability.” *AIChE Journal*, vol. 12, no. 4, 1966, pp. 669–678., https://doi.org/10.1002/aic.690120411.

Hardalupas, Y., and J. H. Whitelaw. “Characteristics of Sprays Produced by Coaxial Airblast Atomizers.” Journal of Propulsion and Power, vol. 10, no. 4, 1994, pp. 453–460., http://doi.org/10.2514/3.23795.

Hewitt, A. J. “Droplet Size Spectra Classification Categories in Aerial Application Scenarios.” Crop Protection, vol. 27, no. 9, 2008, pp. 1284–1288., https://doi.org/10.1016/j.cropro.2008.03.010.

Holland, J. M., et al. “A Comparison of Spinning Disc Atomisers and Flat Fan Pressure Nozzles in Terms of Pesticide Deposition and Biological Efficacy within Cereal Crops.” Crop Protection, vol. 16, no. 2, 1997, pp. 179–185., https://doi.org/10.1016/s0261-2194(96)00071-3.

Jaberi, A., and M. Tadjfar. “Two-Dimensional Liquid Sheet in Transverse Subsonic Airflow.” Experimental Thermal and Fluid Science, vol. 123, 2021, p. 110326., https://doi.org/10.1016/j.expthermflusci.2020.110326.

Jadidi, M., et al. “Breakup of Elliptical Liquid Jets in Gaseous Crossflows at Low Weber Numbers.” Journal of Visualization, vol. 22, no. 2, 2018, pp. 259–271., https://doi.org/10.1007/s12650-018-0537-8.

Kasyap, T.V., et al. “Flow and Breakup Characteristics of Elliptical Liquid Jets.” International Journal of Multiphase Flow, vol. 35, no. 1, 2009, pp. 8–19., https://doi.org/10.1016/j.ijmultiphaseflow.2008.09.002.

Khan, M. A., et al. “First Step towards Atomization at Ultra-Low Flow Rates Using Conventional Twin-Fluid Atomizer.” Experimental Thermal and Fluid Science, vol. 109, 7 June 2019, p. 109844., http://doi:10.1016/j.expthermflusci.2019.109844.

Kozul, M., et al. “Aerodynamically Driven Rupture of a Liquid Film by Turbulent Shear Flow.” *Physical Review Fluids*, vol. 5, no. 12, 2020, https://doi.org/10.1103/physrevfluids.5.124302.

Kumar, A., and S. Sahu. “Influence of Nozzle Geometry on Primary and Large-Scale Instabilities in Coaxial Injectors.” *Chemical Engineering Science*, vol. 221, 2020, p. 115694., https://doi.org/10.1016/j.ces.2020.115694.

Kumar, A., and S. Sahu. “Liquid Jet Breakup Unsteadiness in a Coaxial Air-Blast Atomizer.” International Journal of Spray and Combustion Dynamics, vol. 10, no. 3, 2018, pp. 211–230., https://doi.org/10.1177/1756827718760905.

Lasheras, J. C., et al. “Break-up and Atomization of a Round Water Jet by a High-Speed Annular Air Jet.” Journal of Fluid Mechanics, vol. 357, 1998, pp. 351–379., https://doi.org/10.1017/s0022112097008070.

Lee, J., and K. A. Sallam. “Column Thickness Variation of 100-Mm Liquid Jets in Still Air.” Atomization and Sprays, vol. 27, no. 1, 2017, pp. 31–43., https://doi.org/10.1615/atomizspr.2016016089.

Leroux, B., et al. “Experimental Study of Coaxial Atomizers Scaling. Part i: Dense Core Zone.” Atomization and Sprays, vol. 17, no. 5, 2007, pp. 381–407., https://doi.org/10.1615/atomizspr.v17.i5.10.

Levy, Y., et al. “Study of Two Miniature Air-Assist Atomizers with Radial and Axial Air Swirlers.” Volume 1: Combustion and Fuels, Education, 2006, https://doi.org/10.1115/gt2006-90711.

Lin, S. P., and R. D. Reitz. “Drop and Spray Formation from a Liquid Jet.” *Annual Review of Fluid Mechanics*, vol. 30, no. 1, 1998, pp. 85–105., https://doi.org/10.1146/annurev.fluid.30.1.85.

Liu, H.-F., et al. “Effect of Liquid Jet Diameter on Performance of Coaxial Two-Fluid Airblast Atomizers.” Chemical Engineering and Processing: Process Intensification, vol. 45, no. 4, 2006, pp. 240–245., https://doi.org/10.1016/j.cep.2005.08.003.

Marmottant, P., and E. Villermaux. "On spray formation," Journal of Fluid Mechanics, 498, 2004, pp. 73–111.

Mazallon, J., et al. “Primary Breakup of Nonturbulent Round Liquid Jets in Gas Crossflows.” *Atomization and Sprays*, vol. 9, no. 3, 1999, pp. 291–312., https://doi.org/10.1615/atomizspr.v9.i3.40.

Miller, P. C. H., and M. C. B. Ellis. “Effects of Formulation on Spray Nozzle Performance for Applications from Ground-Based Boom Sprayers.” Crop Protection, vol. 19, no. 8-10, 2000, pp. 609–615., https://doi.org/10.1016/s0261-2194(00)00080-6.

Miller, P. C. H., et al. “Adjuvant Effects on Spray Characteristics and Drift Potential.” *Pesticide Formulations and Application Systems: A New Century for Agricultural Formulations, Twenty First Volume*, 2001, https://doi.org/10.1520/stp10727s.

Murugan, Raju, et al. “Experimental Study of Liquid Spray Mode of Twin Fluid Atomizer Using Optical Diagnostic Tool.” *Flow, Turbulence and Combustion*, vol. 106, no. 1, 2020, pp. 261–289., https://doi.org/10.1007/s10494-020-00195-1.

Payri, R., et al. “Analysis of Diesel Spray Atomization by Means of a near-Nozzle Field Visualization Technique.” *Atomization and Sprays*, vol. 21, no. 9, 2011, pp. 753–774., https://doi.org/10.1615/atomizspr.2012004051.

Porcheron, E., et al. “Effect of Injection Gas Density on Coaxial Liquid Jet Atomization.” Atomization and Sprays, vol. 12, no. 1-3, 2002, pp. 209–228., https://doi.org/10.1615/atomizspr.v12.i123.110.

Rajendran, S., et al. “Experimental Investigation of Jet Breakup at Low Weber Number.” *Atomization and Sprays*, vol. 27, no. 9, 2017, pp. 821–834., https://doi.org/10.1615/atomizspr.2017019424.

Sallam, K. A., and G. M. Faeth. “Surface Properties during Primary Breakup of Turbulent Liquid Jets in Still Air.” *AIAA Journal*, vol. 41, no. 8, 2003, pp. 1514–1524., https://doi.org/10.2514/2.2102.

Sallam, K. A., et al. “Turbulent Primary Breakup of Round and Plane Liquid Jets in Still Air.” 40th AIAA Aerospace Sciences Meeting & Exhibit, 2002, https://doi.org/10.2514/6.2002-1115.

Sallam, K. A., et al. “Breakup of Round Liquid Jets in Gaseous Crossflows.” AIAA Journal 42(12):2529-2540 (2004).

Sikkema, P. H., et al. “Flat Fan and Air Induction Nozzles Affect Soybean Herbicide Efficacy.” Weed Biology and Management, vol. 8, no. 1, 2008, pp. 31–38., https://doi.org/10.1111/j.1445-6664.2007.00271.x.

Soni, S. K., and P. S. Kolhe. “Liquid Jet Breakup and Spray Formation with Annular Swirl Air.” *International Journal of Multiphase Flow*, vol. 134, 2021, p. 103474., https://doi.org/10.1016/j.ijmultiphaseflow.2020.103474.

Tanner, F. X., et al. “Modeling and Simulation of Air-Assist Atomizers with Applications to Food Sprays.” *Applied Mathematical Modelling*, vol. 40, no. 11-12, 2016, pp. 6121–6133., https://doi.org/10.1016/j.apm.2016.01.048.

Thompson, J. C., and Rothstein, J. R. “The Atomization of Viscoelastic Fluids in Flat-Fan and Hollow-Cone Spray Nozzles.” Journal of Non-Newtonian Fluid Mechanics, vol. 147, no. 1-2, 2007, pp. 11–22., https://doi.org/10.1016/j.jnnfm.2007.06.004.

Tian, X.-S., et al. “Liquid Entrainment Behavior at the Nozzle Exit in Coaxial Gas–Liquid Jets.” Chemical Engineering Science, vol. 107, 2014, pp. 93–101., https://doi.org/10.1016/j.ces.2013.12.008.

Uremis, I., et al. “Studies on Different Herbicide Application Methods in Second-Crop Maize Fields.” Crop Protection, vol. 23, no. 11, 2004, pp. 1137–1144., https://doi.org/10.1016/j.cropro.2004.05.004.

Varga, C. M., J. C. Lasheras, E. J. Hopfinger. Initial breakup of a small-diameter liquid jet bya high-speed gas stream. Journal of Fluid Mechanics, Cambridge University Press (CUP), 2003, 497, pp.405-434.

Wachter, S., et al. “Effect of Gas Jet Angle on Primary Breakup and Droplet Size Applying Coaxial Gas-Assisted Atomizers.” International Conference on Liquid Atomization and Spray Systems (ICLASS), vol. 1, no. 1, 2021, https://doi.org/10.2218/iclass.2021.5808.

Wachter, S., et al. “Towards System Pressure Scaling of Gas Assisted Coaxial Burner Nozzles – an Empirical Model.” Applications in Energy and Combustion Science, vol. 5, 2021, p. 100019., https://doi.org/10.1016/j.jaecs.2020.100019.

Wang, M.-R., et al. “Atomization Performance of twin fluid injectors with micro-mixing mechanisms.” Proceedings of ICLASS- Aug.27-Sept.1, 2006, Kyoto, Japan, 2006.

Wang, S., et al. “Modeling Liquid Sheet and Droplet Distribution of Flat-Fan Nozzle.” *International Agricultural Engineering Journal*, vol. 28, no. 1, 2019, pp. 88–99.

Wang, Y., et al. “Experimental Study on the Effects of Spray Inclination on Water Spray Cooling Performance in Non-Boiling Regime.” *Experimental Thermal and Fluid Science*, vol. 34, no. 7, 2010, pp. 933–942., https://doi.org/10.1016/j.expthermflusci.2010.02.010.

Watanawanyoo, P., et al. “Experimental Investigations on Spray Characteristics IN Twin-Fluid Atomizer.” Procedia Engineering, vol. 24, 2011, pp. 866–872., https://doi.org/10.1016/j.proeng.2011.12.416.

Wu, P.-K., and G. M. Faeth. “Onset and End of Drop Formation along the Surface of Turbulent Liquid Jets in Still Gases.” Physics of Fluids, vol. 7, no. 11, 1995, pp. 2915–2917., https://doi.org/10.1063/1.868667.

Yang, L.-J., et al. “Theoretical Atomization Model of a Coaxial Gas–Liquid Jet.” Physics of Fluids, vol. 32, no. 12, 2020, p. 124108., https://doi.org/10.1063/5.0030291.

Yarpuz-Bozdogan, N., and A. M. Bozdogan. “Assessment of Dermal Bystander Exposure in Pesticide Applications Using Different Types of Nozzles.” *Journal of Food, Agriculture and Environment*, vol. 7, no. 2, 2009, pp. 678–682.

Zacarías, A., et al. “Experimental Assessment of Ammonia Adiabatic Absorption into Ammonia–Lithium Nitrate Solution Using a Flat Fan Nozzle.” *Applied Thermal Engineering*, vol. 31, no. 16, 2011, pp. 3569–3579., https://doi.org/10.1016/j.applthermaleng.2011.07.019.

Zhang, F., et al. “Effect of Elevated Pressure on Air-Assisted Primary Atomization of Coaxial Liquid Jets: Basic Research for Entrained Flow Gasification.” *Renewable and Sustainable Energy Reviews*, vol. 134, 2020, p. 110411., https://doi.org/10.1016/j.rser.2020.110411.

Zhang, M., et al. “Breakup of Rectangular Liquid Jets with Controlled Upstream Disturbances.” International Journal of Multiphase Flow, vol. 139, 2021, p. 103621., https://doi.org/10.1016/j.ijmultiphaseflow.2021.103621.

Zhong, H., et al. “Impact of Naled on Honey Bee Apis Mellifera L. Survival and Productivity: Aerial ULV Application Using a Flat-Fan Nozzle System.” Archives of Environmental Contamination and Toxicology, vol. 45, no. 2, 2003, pp. 216–220., https://doi.org/10.1007/s00244-002-0185-8.

APPENDICES

APPENDIX A

CROSSFLOW FIGURES

Additionally, Fan angle was also inspected as a function of the injection pressure (A.1.). Flow visualization for the 1 mm diameter nozzle (A.2 & A.3) and the bags formed due to flapping instability (A.4) are also included in this Appendix.

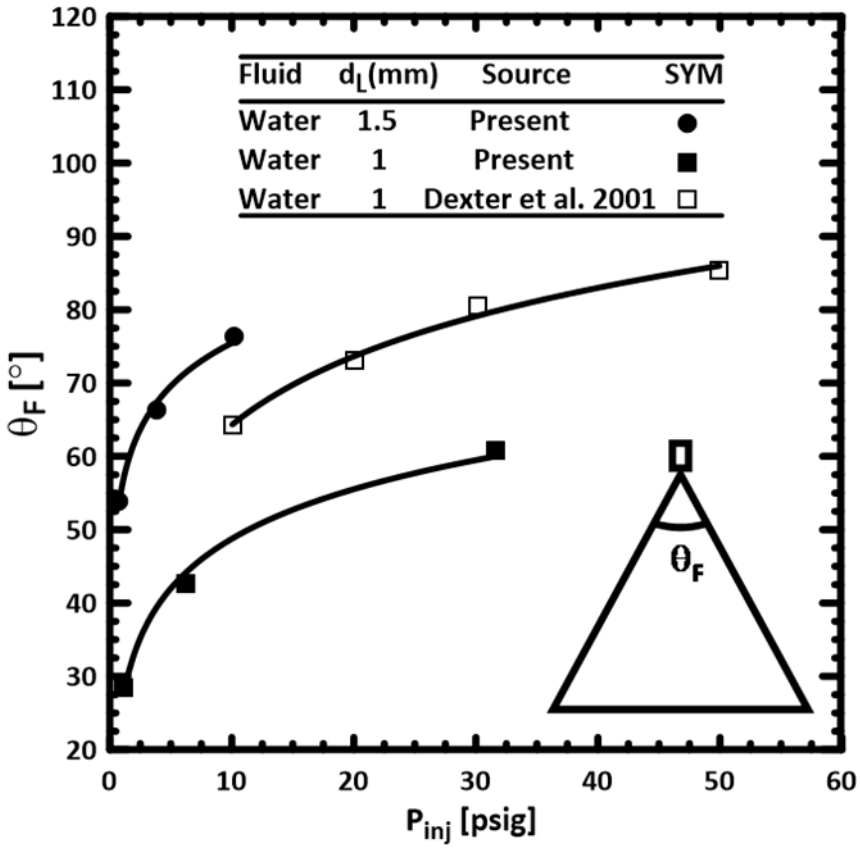

Fig. A.1. Variation of Fan angle as a function of the injection pressure for the two flat fan nozzles used in the present also including the data from (Dexter, 2001).

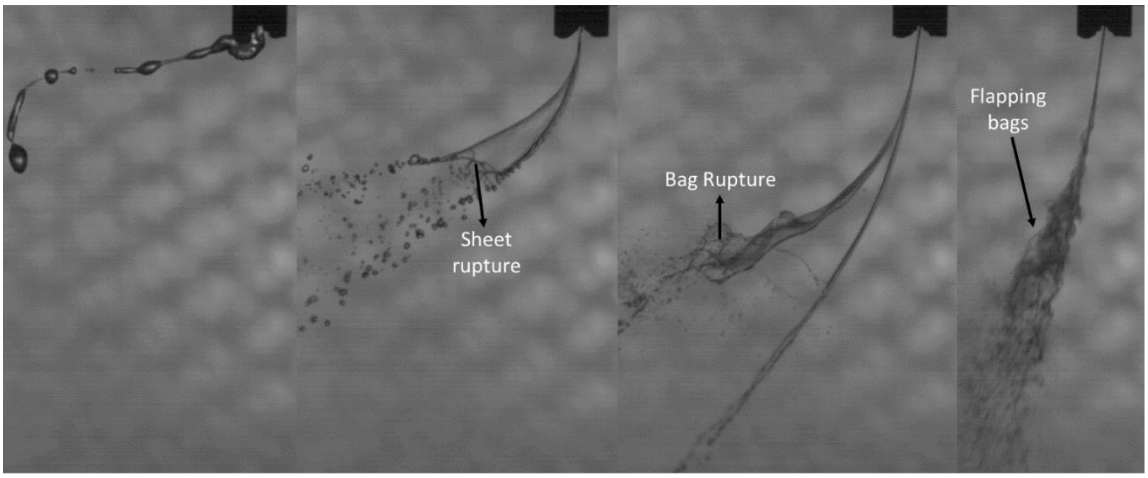

Fig. A.2. Breakup regime visualization showing the effect of jet velocity for the (d_L = 1 mm) nozzle at a crossflow (wind blowing from right to left) velocity of 10.4 m/s.

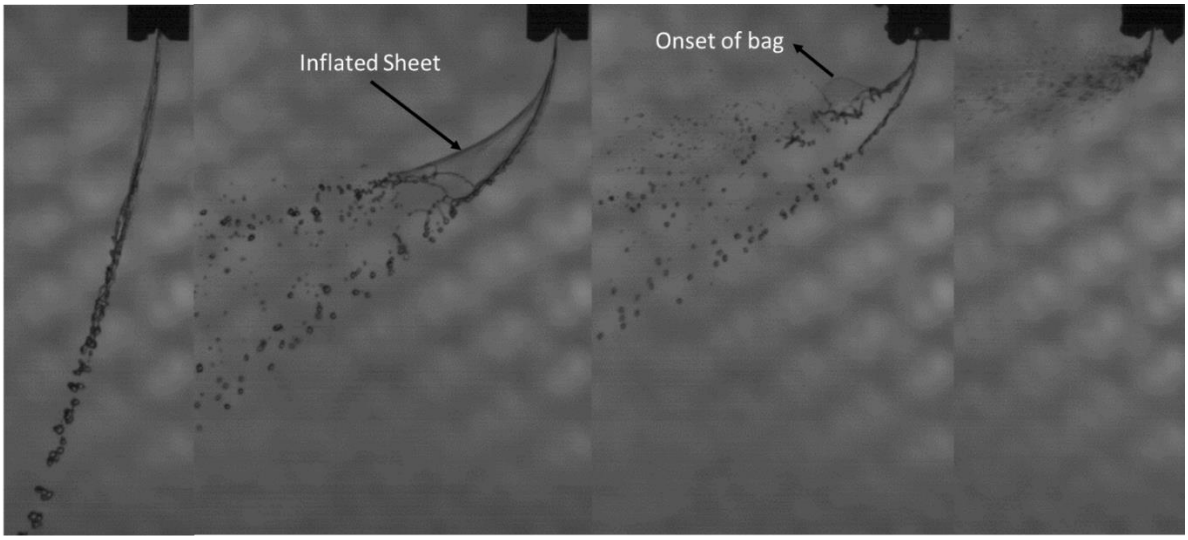

Fig. A.3. Effect of crossflow velocities on flat fan spray (d_L = 1 mm). Test conditions: Liquid exit velocity is 4 m/s.

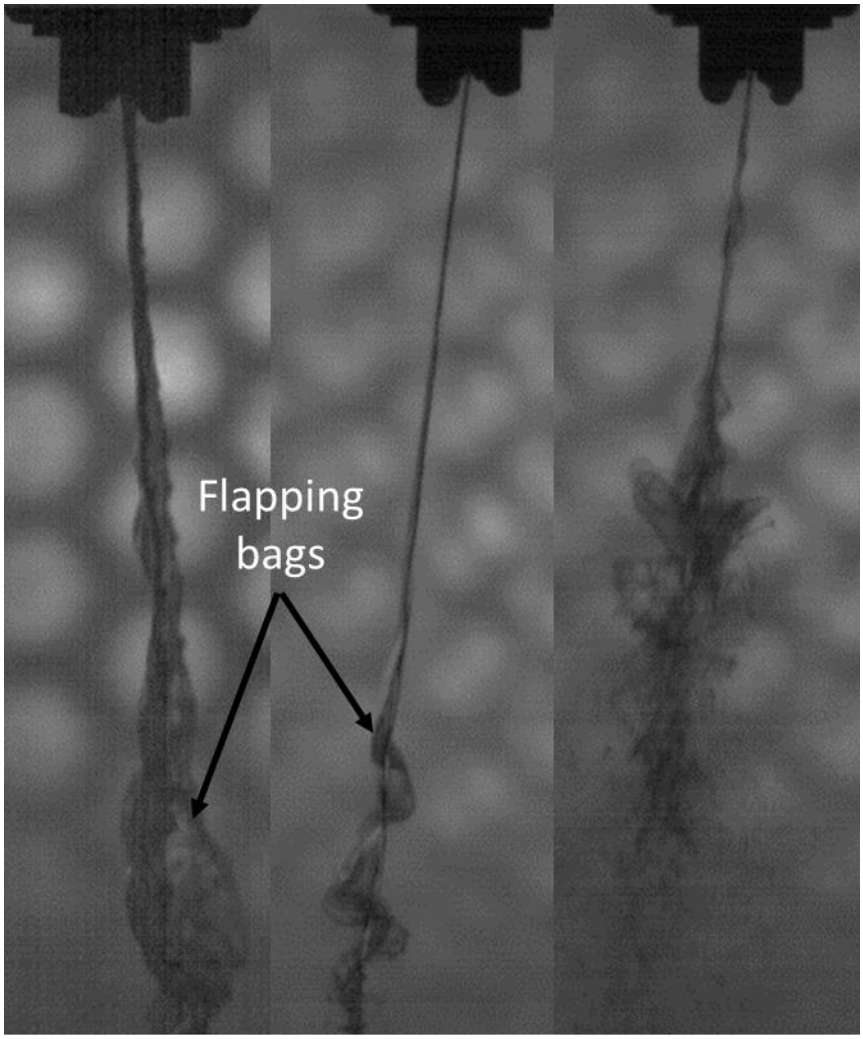

(a) (b) (c)

Fig. A.4. Bags formed because of flapping instability at higher flow rates. (a), (b) no crossflow & (c) with crossflow.

APPENDIX B

COFLOW FIGURES

Deflection angle of the jet was also investigated and plotted as a function of the liquid flow rate and a decreasing trend of the deflection angle was observed with the increasing liquid flow rate as shown below.

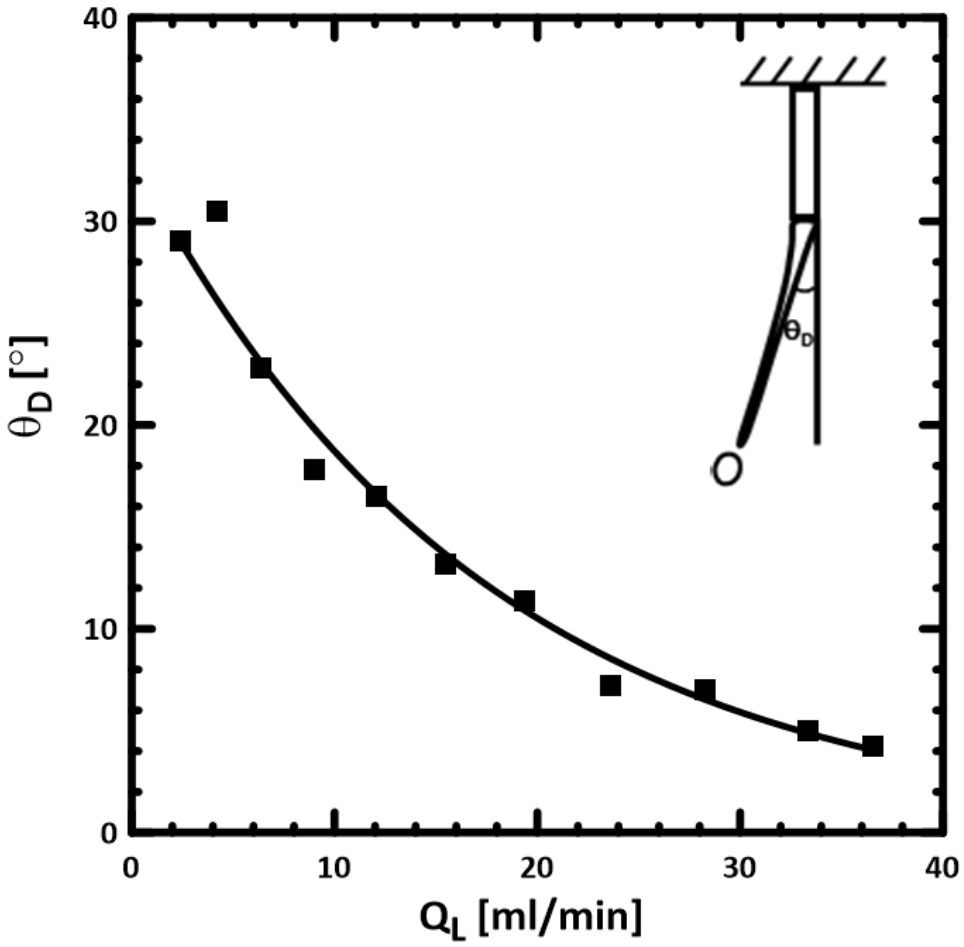

Fig. B.1. Jet deflection angle as a function of the increasing liquid flow rate.

VITA

Muhammad Saqib Raza

Candidate for the Degree of

Master of Science

Thesis: PRIMARY BREAKUP OF LIQUID SHEETS IN CROSSFLOW AND LIQUID JETS IN GASEOUS COFLOW

Major Field: Mechanical and Aerospace Engineering

Biographical:

Education:

Completed the requirements for the Master of Science in Mechanical and Aerospace Engineering at Oklahoma State University, Stillwater, Oklahoma in May, 2022.

Completed the requirements for the Bachelor of Science in Mechanical Engineering at Oklahoma State University, Stillwater, Oklahoma in 2019.

Experience:

Graduate Teaching/Research Assistant.

Intern, New Product Development Center.

Professional Memberships:

American Society of Mechanical Engineers.

Presidents' leadership society, Oklahoma State University.